Annales Societatis Geologorum Poloniae (2016), vol. 86: 185–209. doi: http://dx.doi.org/10.14241/asgp.2016.003

THE PLIOCENE PALUDINA LAKE OF PANNONIAN BASIN: NEW EVIDENCE FROM NORTHERN SERBIA

Ljupko RUNDIĆ[1], Nebojša VASIĆ[2], Dragana ŽIVOTIĆ[3], Achim BECHTEL[4], Slobodan KNEŽEVIĆ[1] & Vesna CVETKOV[5]

[1] University of Belgrade, Faculty of Mining and Geology, Department of Regional Geology, Kamenička 6, 11000 Belgrade, Serbia; emails: ljupko.rundic@rgf.bg.ac.rs, slobodan.knezevic@rgf.bg.ac.rs
[2] University of Belgrade, Faculty of Mining and Geology, Department of Petrology and Geochemistry, Studentski Trg 16, 11000 Belgrade, Serbia; email: nebojsa.vasic@rgf.bg.ac.rs
[3] University of Belgrade, Faculty of Mining and Geology, Department of Economic Geology, Đušina 7, 11000 Belgrade, Serbia; email: dragana.zivotic@rgf.bg.ac.rs
[4] Department of Applied Geosciences and Geophysics, University of Leoben, Peter-Tunner-Str. 5, A-8700 Leoben, Austria; email: achim.bechtel@unileoben.ac.at
[5] University of Belgrade, Faculty of Mining and Geology, Department of Geophysics, Đušina 7, 11000 Belgrade, Serbia; email: vesna.cvetkov@rgf.bg.ac.rs

Rundić, L., Vasić, N., Životić, D., Bechtel, A., Knežević, S. & Cvetkov, V., 2016. The Pliocene Paludina Lake of Pannonian Basin: new evidence from northern Serbia. *Annales Societatis Geologorum Poloniae*, 86: 185–209.

Abstract: This study from the Sremski Karlovci clay pit in northern Serbia sheds new light on the physicochemical conditions, ecology and evolution of the Paludina Lake – the Pliocene successor of the late Miocene giant Lake Pannon hosted by the Pannonian Basin. The multidisciplinary study combines sedimentology, sequence stratigraphy, biostratigraphy, palaeontology, palaeobotany, coal petrology, organic geochemistry and magnetic mineralogy. The sedimentary succession studied represents the lake margin at the foot of the Fruška Gora ridge. Sedimentary facies reveal minor and major lake-level changes, including a forced regression with fluvial valley incision in the succession middle part and the ultimate emergence and covering of the lake floor by Pleistocene loess. Mollusc and ostracod fauna indicates an oligohaline shallow cool-water environment, no deeper than 5–6 m, with an active inflow of spring water. The lake local depth during transgression maxima did not exceed 20 m. Palynological and geochemical analyses indicate a rich and diversified assemblage of gymnosperm plants with a contribution of angiosperms, weeds and microbial biomass in the peat-forming suboxic to oxic coastal swamp environment. Maceral analysis of organic matter shows a prevalence of huminite, accompanied richly by inertinite in lignite and by liptinite in clay. The Pleistocene shift to terrestrial semiarid environment resulted in oxidizing groundwater conditions, with the reddening of sediments around a fluctuating groundwater table and the diagenetic transformation of bacteria-derived greigite into magnetite. In regional stratigraphy, the occurrence of *Viviparus neumayri* Brusina in the lower half of the succession indicates the Lower Paludina Beds of Dacian Stage (early Zanclean age). Other gastropods and certain ostracodes indicate transition to the Middle Paludina Beds of lower Romanian Stage (late Zanclean–early Piacenzian). The upper half of the succession lacks age-diagnostic fossils and is considered to represent Middle Paludina Beds with a possible relic of Upper Paludina Beds at the top.

Key words: Flora, freshwater fauna, lacustrine palaeoenvironment, lignite petrology, organic geochemistry, sedimentary facies.

Manuscript received 5 February 2015, accepted 1 March 2016

INTRODUCTION

The evolution and main geodynamic events of the Pannonian Basin have been investigated extensively during the last two centuries (e.g., see reviews by Balla, 1986; Fodor *et al.*, 1999). The research focused on the reconstruction of changes in the palaeogeographic and palaeoecological conditions controlled by the connectivity of the basin to the world ocean during the Miocene. Less clear is the last stage of the basin evolution, which involved development of a lake system in the latest Miocene to early Pliocene (Magyar *et al.*, 1999; Ter Borgh *et al.*, 2013). Disputed issues include the exact stratigraphic position of these young Lake Pannon deposits and the regional occurrence of Pontian Stage (i.e., the upper Pannonian Stage *sensu lato*) or its equivalents in the Pannonian realm. Most researchers from countries in the central and western parts of the Pannonian Plain deny presence of the Pontian *sensu stricto* (Sacchi and Horvath,

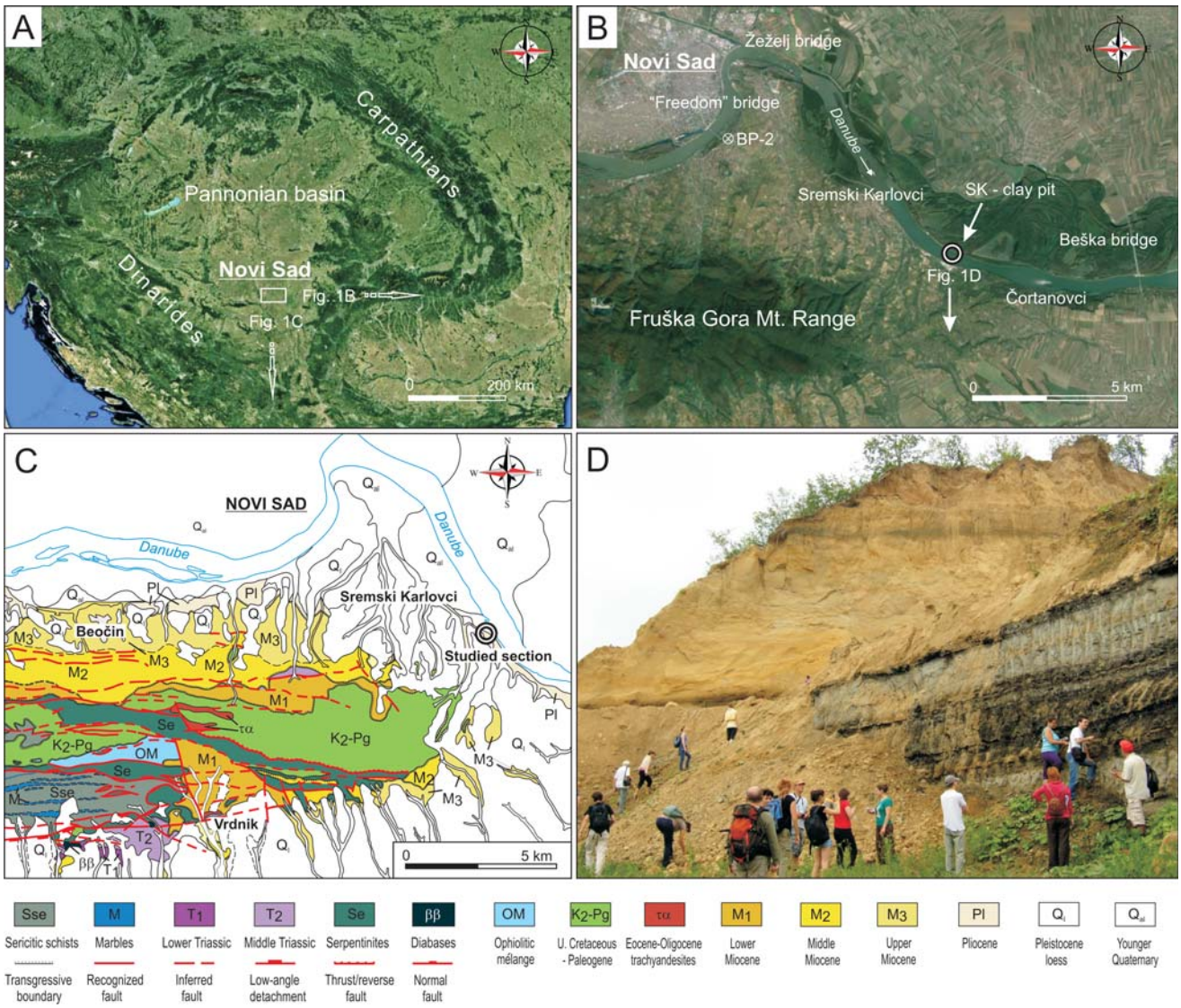

Fig. 1. Location of the study area. **A.** Satellite image of the Pannonian Basin and its surroundings (from Google Earth website) showing the regional location of the present-study area. **B.** Satellite image of the study area (from Google Earth website) showing the Fruška Gora mountain ridge, the Danube River and the localities referred to in the text, including the Sremski Karlovci (SK) clay pit. **C.** Simplified geological map of the eastern part of the Fruška Gora mountain ridge (modified from Čičulić-Trifunović and Rakić, 1971; and Toljić *et al.*, 2013) with the location of the studied outcrop section in the Sremski Karlovci clay pit. **D.** Outcrop photograph of a portion of the Sremski Karlovci clay pit.

2002). Conversely, many stratigraphers from Serbia and Romania consider the last connection between the Central and Eastern Paratethys to correspond to the Pontiazn time (Andreescu *et al.*, 2013). To resolve this controversy, an integrated stratigraphic research is needed for the southern part of the Pannonian Basin in Croatia, Bosnia and Serbia (cf. Harzhauser and Mandic, 2008; Ter Borgh *et al.*, 2013).

The Pannonian Basin developed as a large post-rift thermal sag depression that underwent tectonic inversion in the late Miocene to Quaternary (Fodor *et al.*, 1999; Toljić *et al.*, 2013), which resulted in significant reduction of the long-lived Lake Pannon (Magyar *et al.*, 1999; Bada et al., 2007; Marović *et al.*, 2007). The small successor lake system occupied the area of Croatia, Bosnia, Serbia and a small western part of Romania (Magyar *et al.*, 1999; Mandic *et al.*, 2012). Since the second half of the 19th century, this lake system has been called the Paludina Lake (Neumayr and Paul, 1875), named after the endemic lake-swamp gastropod genus *Vivipara* (= *Paludina*). Main pioneering studies include Neumayr (1869, 1880), Brusina (1870, 1874, 1878, 1882, 1884, 1896, 1902), Herbich and Neumayr (1875), Neumayr and Paul (1875) and Fontannes (1886). The lake-fill sedimentary succession had come to be referred to broadly as the Paludina Beds in the regional literature.

More than a century later, Harzhauser and Mandic (2008) described 183 gastropod species within the 29 genera that inhabited the lake, which they referred to as Lake Slavonia. According to these latter authors, the dominant fauna belonged to the families Melanopsidae (42 species), Viviparidae (35 species), and Hydrobiidae (28 species). The succession has been subdivided into the Lower, Middle and Upper Paludina Beds. The Lower Paludina Beds are charac-

terized by the smoothest forms of genus *Vivipara*, which are stratigraphically succeeded by ribbed forms in the Middle Paludina Beds and highly ornamented forms in the Upper Paludina Beds (Posilović and Bajraktarević, 2010 and references therein). This stratigraphic trend reflects a continuous development of shell ornamentation from ancestral *V. neumayri* with a smooth shell to *V. ornatus* with a spiral ribbed shell. Croatian, Bosnian and Serbian geologists have generally considered the Paludina Beds to be equivalent of the early Pliocene Dacian Stage in the Eastern Paratethyan regional stratigraphy (Andreescu *et al.*, 2013), corresponding to the Zanclean Stage (5.3–3.7 Ma) in the Mediterranean stratigraphy (Cohen *et al.*, 2013). However, high-resolution stratigraphy and geochronology of the Paludina Beds succession remained to be established.

The aim of the present multidisciplinary study is to clarify the stratigraphic position of the Paludina Beds in the regional development and general stratigraphy of the Pannonian Basin. The approach used here integrates sedimentological, petrological, palaeontological and palaeomagnetic methods. The study focuses on outcrop section in the Sremski Karlovci clay pit to the south-east of Novi Sad in Serbia (Fig. 1), and the results shed a new light on the evolution of the ancient Paludina Lake in this southern part of the Pannonian Basin.

GEOLOGICAL SETTING

The Pannonian Basin is a large intracratonic basin developed on the Carpathian-Pannonian microplate surrounded by the Alpine orogenic belts of the Carpathians, Eastern Alps and Dinarides (Fig. 1A). Miocene tectonic extension of the hosting crustal plate in back-arc regime was followed by its tectonic contraction in the Pliocene and Quaternary, since *ca.* 20 Ma (Horvath *et al.*, 2006; Schmid *et al.*, 2008; Ter Borgh *et al.*, 2013). The Fruška Gora mountain belt along the southern margin of the Pannonian Basin (Fig. 1B, C) is the suture zone of the Pannonian and Dinaric crustal blocks (Toljić *et al.*, 2013). This E-trending inselberg horst, flanked by Miocene–Quaternary deposits, provides geological evidence of a late Jurassic obduction of ophiolite-bearing accretionary prism, further Cretaceous subduction and an end-Cretaceous to Eocene collision of the crustal blocks, followed by Miocene uplift and extension of the Pannonian craton (Cloetingh *et al.,* 2006; Horváth *et al.*, 2006; Toljić *et al.*, 2013). The tectonic extension, accompanied by volcanism, was coeval with the uplift of the surrounding Alpine orogenic belts, which largely separated the epicontinental Paratethyan domain from the Mediterranean oceanic Tethyan domain (Rögl, ne1999; Schmid *et al.*, 2008).

The early to middle Miocene pre- and syn-rift deposits in the Pannonian Basin show a transition from continental alluvial-lacustrine to fully marine environments (Ter Borgh *et al.*, 2013). The peak of extensional tectonics was reached in the Badenian–Sarmatian rifting phase (*ca.* 15–11 Ma) at the Great Hungarian Plain adjacent to the Fruška Gora mountain range (Fodor *et al.*, 1999). The long-lived Lake Pannon formed at the middle/late Miocene boundary (*ca.* 11.6 Ma) as a consequence of the tectonic uplift of the Carpathians that separated the basin from marine influences (Magyar *et al.*, 1999; Ter Borgh *et al.*, 2013; Sztanó *et al.*, 2015). It took more than 7 Ma for the large Pannonian Basin to be filled with lacustrine and fluvio-deltaic sediments derived by erosion of the surrounding orogenic belts (Magyar *et al.*, 2013; Radivojević *et al.*, 2014). At the beginning of Pliocene, the semi-brackish giant Lake Pannon became reduced to the much smaller but freshwater Paludina Lake, (Magyar *et al.*, 1999; Harzhauser and Mandic, 2008; Sztanó *et al.*, 2015). The Fruška Gora mountain ridge acted as an elongate island, with lake-margin and swamp environments formed along its shoreline. The Pliocene–Quaternary tectonic compression reactivated some older faults (Fig. 1C), whereby the Paludina Beds were differentially displaced and lost lateral continuity (Toljić *et al.*, 2013). As a result, the Paludina Beds are exposed at different altitudes on the northern and southern flanks of the Fruška Gora horst structure.

The existing knowledge of the Paludina Beds derives mainly from outcrop sections on the flanks of the Fruška Gora mountain range, particularly its northern flank (Janković, 1970, 1977, 1995; Čičulić-Trifunović and Rakić, 1971; Petković *et al.*, 1976; Krstić and Knežević, 2003; Rundić *et al.*, 2011). Best outcrops are in the local sand pits and brick-factory clay pits along the right-hand bank of the Danube River, including the vicinity of Sremski Karlovci (Fig. 1B). In these outcrops, the Lower Paludina Beds – identified by the presence of *Viviparus neumayri* Brusina – are heterolithic deposits comprising sand intercalated with mud, clay and thin lignite layers, although the succession at some localities contains only sand (Rundić *et al.*, 2011). An evidence of younger fossil assemblages, especially gastropods and ostracods, in the uppermost part of these outcrops indicates the presence of Middle Paludina Beds. The Upper Paludina Beds have not been recognized in surface outcrops and are considered as non-preserved (Krstić, 2006), but are known from boreholes on the left-hand bank of the Danube River and farther north in the Banat–Bačka area of northern Serbia, where they reach a thickness of more than 200 m (Krstić, 2006). The upward transition of Pontian sands, the youngest Miocene deposits in the area, to the muddy lacustrine facies of Paludina Beds is similarly known only from boreholes near Beočin (Fig. 1C) (Petković *et al.*, 1976; Krstić, 2006). The Paludina Beds in the whole area are overlain unconformably by Quaternary deposits, typically Pleistocene loess with palaeosol horizons (Krstić, 2006).

The Sremski Karlovci clay pit (Fig. 1D; N 45°10′50″, E 19°57′50″) on the right-hand bank of the Danube River, downstream of the town of Sremski Karlovci (Fig. 1B, C), affords a relatively small but palaeogeographically unique outcrop of the Paludina Beds. This open-pit site is located at the north-eastern extremity of the Fruška Gora foot-plain, where the Pliocene lake-margin deposits are accessible in relatively few isolated outcrops (Čičulić-Trifunović and Rakić, 1971; Toljić *et al.*, 2013). The lacustrine Paludina Beds at the Sremski Karlovci pit are underlain by sands, probably a transition from the topmost Pontian sands known from nearby boreholes (Krstić, 2006; Krstić *et al.*, 2013), and are covered with Pleistocene loess (Fig. 1C). Coeval late Pontian lacustrine muddy deposits with numerous pelecypods, including *Limnocardium zagrabiense* Brusina, are known

from outcrops at the Danube River bank near the railway station of Sremski Karlovci and near the river bridge at Beška (Fig. 1B) – both sites only a few more kilometres away to the north and east, respectively, from the Fruška Gora palaeo-island. The shoreline of Paludina Lake would thus appear to have transgressively overstepped the late Pontian shoreline of the old Lake Pannon.

MATERIAL AND METHODS

Lithostratigraphic logging and sampling of the sedimentary succession in the Sremski Karlovci clay pit (Fig. 1D) was conducted, with a total of twenty-three samples (*ca*. 500 g each) labelled SK-1 to SK-22 and PM-1 (Fig. 2). All the samples were split in the laboratory for different kinds of analysis.

Palaeontological analysis of 22 samples (SK-1 to SK-22) was performed after their washing in warm water and subsequent sieving (meshes 0.6–0.125 mm). Ostracodes appeared to be well preserved and were picked up completely or partially, depending on their abundance in a sample, as only a few samples had high ostracode content with both adult and juvenile forms. Molluscs were collected from several samples and – after a standard cleaning – some of the specimens were further treated with a one-minute ultrasound bath. Microphotographs were obtained by using a JEOL JSM-6610LV scanning electron microscope (SEM) at the Faculty of Mining and Geology, University of Belgrade. Prior to their SEM analysis, all specimens were gold-coated (film thickness *ca.* 20 nm) in argon atmosphere using a Leica EM SCD005 sputter coater. Primary electron beam with Ib of 0.7 nA and acceleration voltage of 5 kV was used to obtain SEM images in secondary electron mode. All of the fossil specimens are stored in the Department of Regional Geology, Faculty of Mining and Geology, University of Belgrade (collection code 2013IGSK1-22).

For maceral analysis, the samples of lignite (SK-5 and SK-11, Table 1) and coaly clay (SK-12 and SK-14) were crushed to a maximum particle size of 1 mm, mounted in epoxy resin and then polished (ISO, 2009a). Analysis was performed on a Leitz DMLP microscope with monochromatic and UV light illumination on 500 points (ISO, 2009b). The maceral description follows the terminology developed by the International Committee for Coal and Organic Petrology for huminite (Sykorova *et al.*, 2005), liptinite (Taylor *et al.*, 1998) and inertinite (ICCP, 2001).

Reflectance measurements were performed under a monochromatic light of 546 nm using a Leitz DMRX microscope (Leica MPV) and optical standards with reflectance values of 0.899% and 1.699% in oil, following the procedures outlined by ISO (2009c). The rank was determined by measuring the random reflectance on ulminite B. The total organic carbon (TOC) content was determined with a Vario EL III CHNS/O Elemental Analyzer of Elementar Analysensysteme GmbH on samples pre-treated with hydrochloric acid (1:3, v/v).

For organic geochemical analyses, representative portions of selected samples were extracted for *ca.* 1 hour by using dichloromethane in a Dionex ASE 200 accelerated solvent extractor at 75 °C and 50 bars. After evaporation of the solvent to 0.5 ml of total solution in a Zymark TurboVap 500 closed-cell concentrator, asphaltenes were precipitated from an 80:1 hexane-dichloromethane solution and separated using centrifugation. The hexane-soluble fractions were separated into NSO compounds, saturated hydrocarbons and aromatic hydrocarbons using medium-pressure liquid chromatography (MPLC) with a Köhnen-Willsch instrument (Radke *et al.*, 1980).

The saturated and aromatic hydrocarbon fractions were analysed on a gas chromatograph equipped with a 30-m DB-5MS fused silica capillary column (inside diameter 0.25 mm, film thickness 0.25 μm) and coupled to a Finnigan MAT GCQ ion-trap mass spectrometer (GC–MS system). The oven temperature was programmed to increase from 70 °C to 300 °C at 4 °C/min, followed by an isothermal period of 15 minutes. Helium was used as the carrier gas. The sample was injected splitless with the injector temperature of 275 °C. The spectrometer was operated in the EI (electron ionization) mode over a scan m/z range from 50 to 650 (0.7 s total scan time). The data were processed with a Finnigan data system. Individual compounds were identified on the basis of retention time in the total ion current (TIC) chromatogram and a comparison of the mass spectra with published data. The relative percentages and absolute concentrations of different compound groups in the saturated and aromatic hydrocarbon fractions were calculated by using peaks of the TIC chromatograms in relation to those of internal standards (deuterated *n*-tetracosane and 1.1'-binaphthyl, respectively), or by an integration of peak areas in mass chromatograms with the response factor used to correct for the intensities of fragment ion in quantification of the total ion abundance. The concentrations were normalized to TOC.

For magnetic mineralogy measurements, fresh clay samples were collected in two places directly above a lignite layer (sample PM-1, Fig. 2). The samples were subjected to magnetic experiments which included progressive acquisition of saturation isothermal remanent magnetization (IRM) up to the maximum field of 2.94 T and a stepwise thermal demagnetization of three-component IRM (Lowrie, 1990) to identify the ferromagnetic mineral components. IRM acquisition was conducted using an MMPM10 pulse magnetizer. Thermal demagnetization was performed in a MMTD80 oven, and the direction and intensity of RM were measured by using a JR-5 spinner magnetometer. The low-field magnetic susceptibility was measured after each step of heating by using a MFK1-A kappabridge.

RESEARCH RESULTS

Sedimentological analysis

The succession of Pliocene deposits exposed in the Sremski Karlovci clay pit has a measured thickness of 34.3 m and is covered with a layer of Pleistocene loess (Fig. 2). The succession has been divided into four main sedimentary units, which differ markedly from one another and are referred to broadly as lithofacies A–D (Fig. 2). These four successive lithofacies are described and interpreted in the present section.

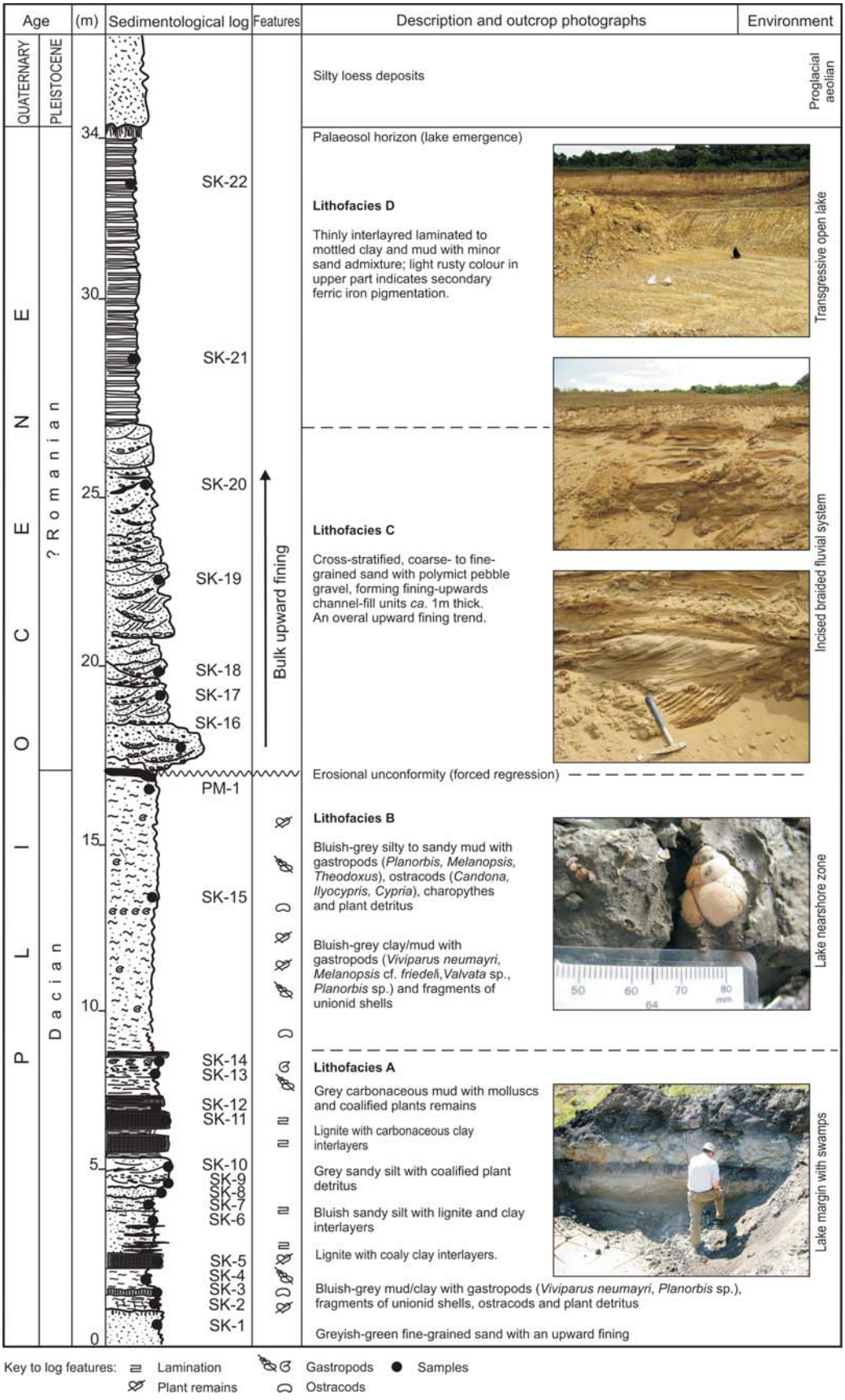

Fig. 2. Sedimentological log of the succession exposed in the Sremski Karlovci clay pit (Fig. 1), with a brief description of main lithofacies, their outcrop photographs and environmental interpretation. Samples SK 1–22 were subject to a range of laboratory analyses; sample PM-1 was subject to palaeomagnetic investigation.

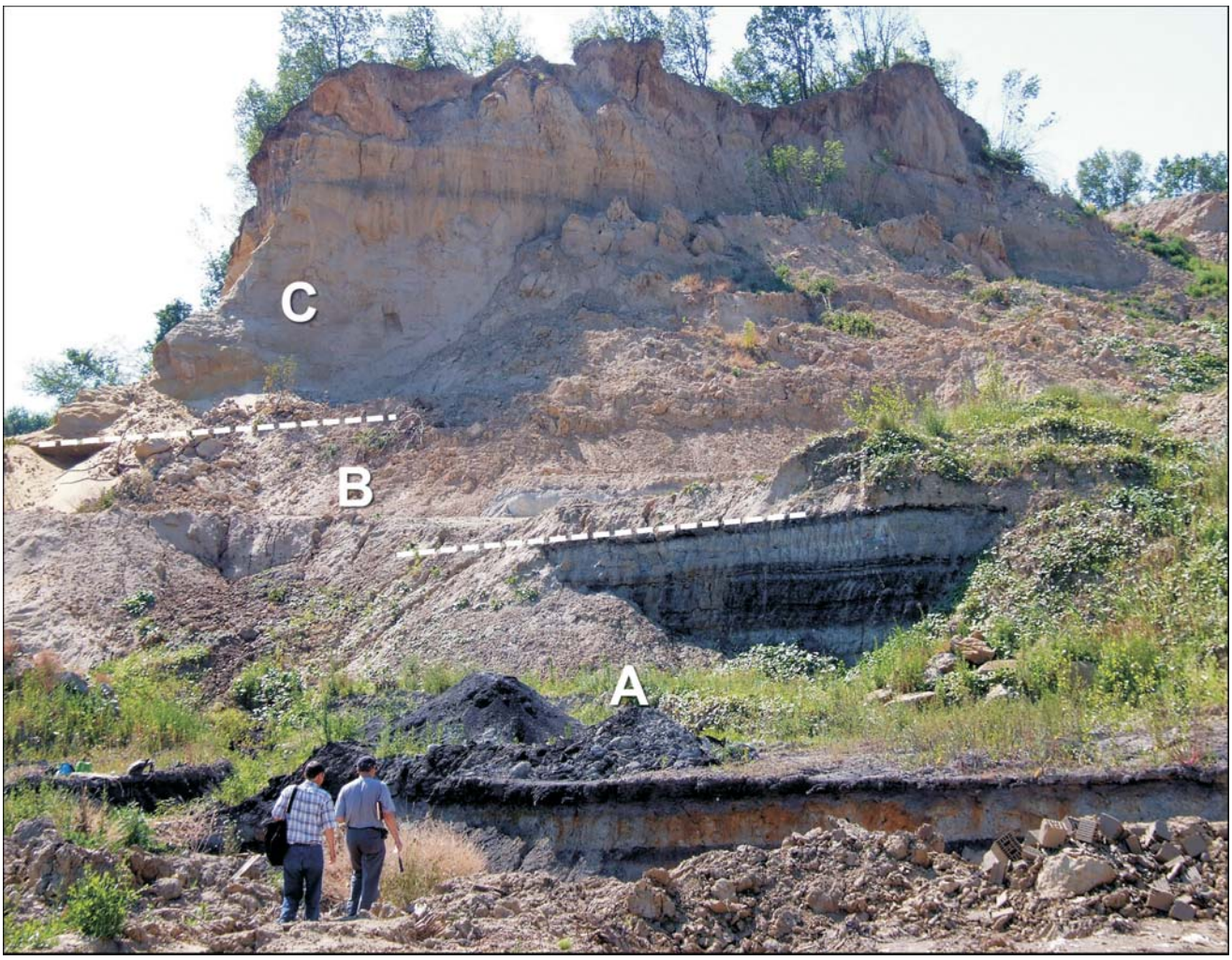

Fig. 3. Outcrop in the Sremski Karlovci clay pit showing the vertically superimposed deposits of lithofacies A, B and C (see log in Fig. 2). The muddy lacustrine deposits of lithofacies B are here deeply incised by the fluvial lithofacies C and only *ca.* 4 m thick, but laterally reach a thickness of at least 12 m within the open-pit outcrop section.

Lithofacies A

Description: This lowest unit, with an exposed thickness of 8.3 m (Fig. 2), is quite heterolithic, showing an alternation of sand, silt, mud, clay and coaly clay, with three lignite seams up to 0.8 m thick (Figs. 3 and 4). Sand has a mean grain size in the range of 0.07–0.43 mm and dominates in the basal part, showing moderate sorting and ripple cross-lamination. Silt and mud layers are planar parallel laminated, containing coalified plant remains and whole or fragmented gastropod and mollusc shells. Ostracode remains are visible on the surface of some samples (SK-2 and SK-3, Fig. 2). The unit as a whole shows an overall upward fining from sandy basal part to the silt-dominated middle part and muddy upper part intercalated with lignite layers.

Interpretation: The heterolithic deposits of lithofacies A, with lignite seams and carbonaceous mud/clay layers, indicate a lake-margin environment hosting swamps. Phytogenic deposits indicate anoxic conditions (Ielpi, 2012), which is supported by the occurrence of pyrite. The overall upward fining and transition to the overlying muddy litho-f acies B (Fig. 2) indicate a gradual lake expansion. The transgression apparently transformed the lake margin from an open shore with active fluvio-deltaic sand supply into a fluctuating and increasingly muddy environment with episodic encroachment of swamp vegetation and anoxia.

Lithofacies B

Description: This next, higher unit (Figs 2, 3) is *ca.* 9 m thick and consists of bluish-grey clay/mud, mainly massive, passing upwards into a better laminated silty to sandy mud. The lithologically monotonous unit contains isolated lenticular aggregates of mollusc shells, particularly coquinas of freshwater snails such as *Melanopsis*, *Planorbis* and *Viviparus*. The fauna specimens are generally of small size (up to 1 cm), except for a few viviparids that exceed slightly 2 cm in size. The index species *Viviparus neumayri* Brusina was found at the base of the unit. There are also scattered plant remains, fragments of freshwater unionid mussels and rare ostracodes (*Candona*, *Ilyocypris*, *Cypria*). This litho-f acies unit has a sharp, erosional contact with the overlying coarse-grained lithofacies C.

Interpretation: The muddy lithofacies B indicates a standing-water nearshore lake environment dominated by hemipelagic suspension fallout, probably fluctuating due to

the superficial boosting of water turbulence by storm waves. Scattered plant detritus and the lack of significant sand supply suggest a vegetated swampy shoreline without an active clastic beach zone or coastal fluvio-deltaic system. Deposition of massive mud is attributed to an intense sediment fallout by clay flocculation, rather than to bioturbation (Basilici, 1997; Ielpi, 2012), taking into account that the burial and compaction significantly obscure initial fabric (Allen, 1985). Laminated or thinly banded mud may indicate spasmodic delivery of wind-blown silt, transient alongshore drift of storm- or river-generated suspension plumes, and possibly local pulsating underflows of fluid mud (Traykovski *et al.*, 2000; Cohen, 2003; Ichaso and Dalrymple, 2009; Ielpi, 2012).

Lithofacies C

Description: This third sedimentary unit is *ca.* 10 m thick, has a distinctly erosional base and consists of coarse-grained clastic deposits (Figs 2, 3). The deposits form scour-based fining-upwards packages, up to around 1 m thick, composed of sandy pebble gravel or pebbly sand passing upwards into coarse-grained to medium- or fine-grained sand (Fig. 5). Each such package shows trough cross-stratification (Fig. 6), locally overlain by ripple cross-lamination in fine sand. Sand is fairly well sorted, with a mean grain size of 0.26–1.06 mm. Some of the packages are draped with a thin relic mud layer. Gravel is subrounded and polymictic, containing some calcareous mud intraclasts. Fossil fauna is lacking.

Fig. 4. Close-up outcrop detail of the lake-margin lithofacies A (Fig. 2), showing: 1 – medium- to fine-grained sand with tiny carbonate concretions and carbonized flora; 2 – three lignite beds interlayered with coaly clay; 3 – clay, partly coaly, rich in mollusc moulds and carbonized swamp plant fragments; 4 – coaly clay layer; and 5 – bluish-grey clay layer above.

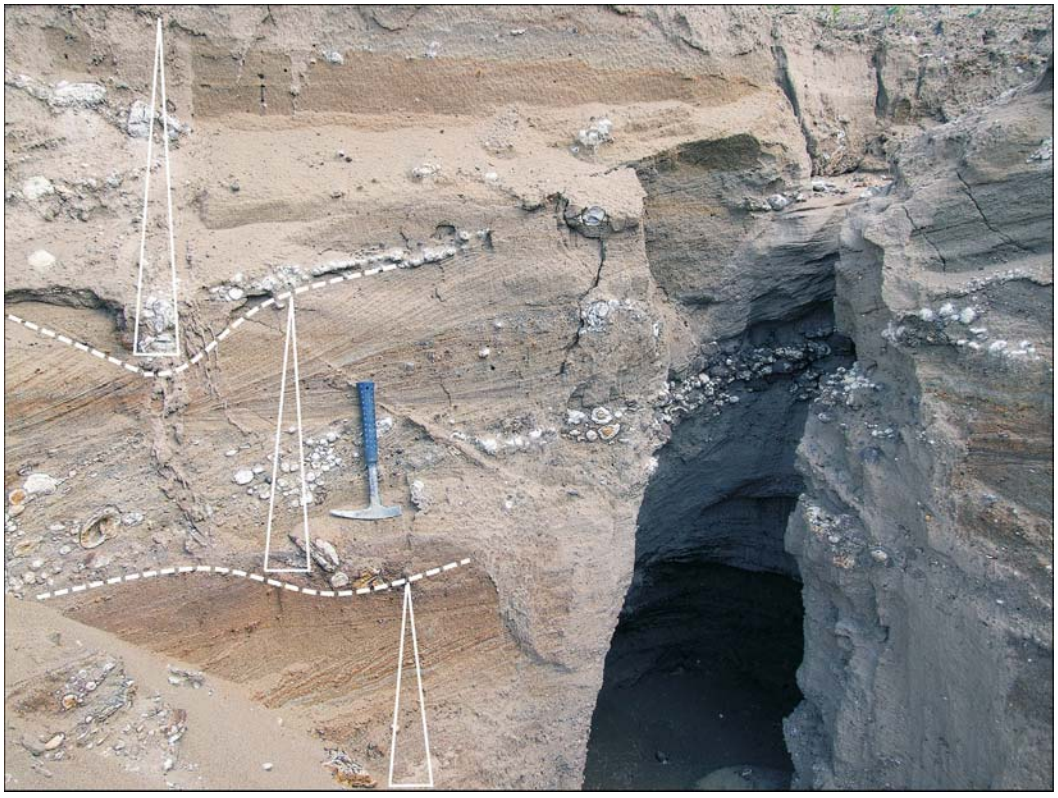

Fig. 5. Outcrop detail of the lower part of lithofacies C (Fig. 2), showing erosionally-stacked fining-upwards gravelly sand packages with trough cross-stratification interpreted as fluvial braided channel-fill deposits. The gravel component is extraformational and polymictic, but includes intraformational mud clasts.

Fig. 6. Close-up outcrop detail of lithofacies C (Fig. 2) showing trough cross-strata sets stacked into a mounded package interpreted as a fluvial mid-channel braid bar.

Interpretation: The coarse-grained lithofacies C signifies a dramatic change of sedimentary environment. The scour-based, cross-stratified sediment packages are channel-fill deposits. Their offset erosional stacking (Fig. 5) indicates a system of laterally mobile braided-stream channels *ca.* 1 m deep (cf. Miall, 1996). Mounded packages of trough cross-stratification (Fig. 6) indicate stacking of linguoid 3D dunes as mid-channel or side bars (cf. Allen, 1983). Sparse lenticular mud layers are relic slack-water deposits of channel abandonment phases. The basal erosional unconformity separating lithofacies C from the underlying lacustrine lithofacies B (Fig. 2) indicates a lake forced regression, with the fluvial system cutting across an emerging lake margin and probably forming an incised valley. An associated coeval lowstand delta (Catuneanu, 2006) must have formed at the lake fallen shoreline to the north-east. The overall fining-upwards trend of lithofacies C and its upward transition into lacustrine lithofacies D indicate a transgressive systems tract (Catuneanu, 2006) signifying a new episode of the lake relative level rise and expansion.

Lithofacies D

Description: This upper sedimentary unit is up to 7 m thick (Fig. 2) and consists of variegated muddy deposits, comprising thinly interlayered clay, silty to sandy mud and subordinate fine-grained sand. Argillaceous layers are parallel-laminated to mottled and yellowish- to reddish-grey in colour. Sandy layers have a stronger rusty-red hue. No fossils have been found in this lithofacies unit. It is covered with a palaeosol horizon and overlain by typical loess deposits, well known from the Pleistocene in the region.

Interpretation: The monotonous muddy deposits of lithofacies D indicate an offshore lake environment with a varying input of silt and fine sand, probably due to frequent storm events. Lithofacies D overlies conformably the fluvial lithofacies C, which implies lake expansion and major regional transgression. Lake expansion would increase the wave fetch and hence the impact of wind on the lake water column. There is no evidence of anoxia, which supports the notion of well-oxygenated lake bottom waters (Potter *et al.*, 2005; Ielpi, 2012). The lake area in this part of the region was eventually emerged and vegetated before being covered by Pleistocene loess, which implies a prolonged period of terrestrial conditions. A fluctuating groundwater table during this period might explain the reddening of sediment (Walker, 1967, 1973, 1974; Walker and Honea, 1969) and probable disappearance of fauna shells by dissolution (Crenshaw, 1980).

Fossil fauna and flora

For more than a century, the biostratigraphy of the Paludina Lake has been based on viviparid gastropods. A viviparid phylogenetic tree was first described by Neumayr and Paul (1875) from the Paludina Beds in Croatia's Slavonia on the basis of shell morphology and stratigraphic distribution. These Pliocene freshwater sands and muds represent the final stages of lacustrine sedimentation in the Pannonian Basin and bear a valuable record of viviparid shell evolution, most notably the increasing shell ornamentation and development of spiral rib forms (Posilović and Bajraktarević, 2010).

In the present case, abundant fossils occur in the lower half of the sedimentary succession – in its lithofacies A and B (samples SK-2, SK-3 and SK-13 to SK-15, Fig. 2). The richest fossil assemblages are found in the bluish-grey mud beds (e.g., sample SK-15), which contain imprints of poorly preserved thin bivalves, moulds of gastropods, fragments of freshwater unionid shells, ostracods, plant detritus and charophytes. The occurrence of index species *Viviparus neumayri* Brusina indicates that the deposits represent the Lower Paludina Beds, which means the Dacian Stage (Zan-

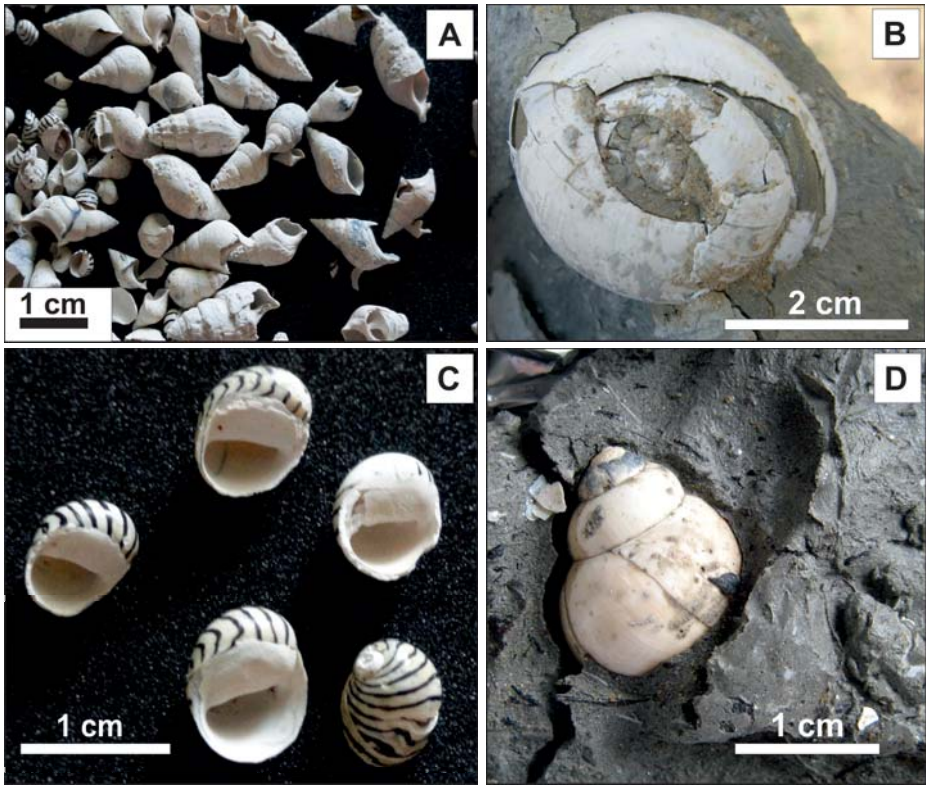

Fig. 7. Fossil fauna in the lower half of the Sremski Karlovci outcrop section (Fig. 2). **A.** Small gastropods dominated by specimens of *Melanopsis* sp. up to *ca.* 2 cm in size, from sample SK-15. **B.** *Planorbi*s sp. **C.** *Theodoxus* cf. *slavonicus* Brusina, with the largest specimen less than 1 cm in size. **D.** *Viviparus neumayri* Brusina.

clean) of the lower Pliocene (Janković, 1977, 1995; Krstić, 2006). The fossil molluscs are dominated by the following forms (Figs 7 and 8): *V. neumayri* Brusina, *V.* cf. *suessi* Neumayr, *Lithoglyphus acutus decipiens* Brusina, *Melanopsis recurens* Neumayr, *M. lanceolata* Neumayr, *M.* cf. *slavonica* Brusina, *M.* cf. *friedeli* Brusina, *Hydrobia longaeva* Neumayr, *Gyraulus* sp., *Planorbis* sp., *Theodoxus semiplicatus* Neumayr, *T.* cf. *rumanus* Sabba, *T.* cf. *slavonicus* Brusina., *Dreissena polymorpha* Pallas, *Valvata* sp., *Bithynia* sp., *Anisus* sp., *Carychium* sp. and fragments of unionid *Psilunio* sp.

The gastropod families Melanopsidae and Planorbidae dominate, making up more than 75% of total molluscs. Predominant are Melanopsidae, mostly small forms up to 1–2 cm in size (Fig. 7A), although sample SK-15 appeared to contain also numerous poorly preserved specimens of larger (3 cm) species from family Planorbidae (Fig. 7B). The Planorbidae have thin brittle shells and hence occur mainly as coquinas. Other gastropods, such as *Bithynia* and *Theodoxus*, are even smaller, less than 0.5 cm in size (Fig. 7C). Only two species of viviparids have been found, but one is the index species *V. neumayri* Brusina (Fig. 7D) (Janković, 1977, 1995; Posilović and Bajraktarević, 2010). In addition to the typical lacustrine and swamp/marsh gastropod species, such as *Viviparus* and *Melanopsis*, some aquatic (*Gyraulus* sp., *Planorbis* sp.) and terrestrial pulmonates (*Carychium* sp.) were found (Krstić, 2006). Except for the widespread and well-preserved *Theodoxus*, gastropod species are scarce in the samples.

Scarce also, relative to molluscs, are ostracodes, although some samples (SK-2, SK-14 and SK-15, Fig. 2) appeared to contain abundant assemblages of lacustrine and freshwater ostracod species (see also Gagić and Sokač, 1972; Krstić, 2006). Best represented in all samples are genera *Candona* and *Ilyocypris*, whereas other species (*Candonopsis*, *Cyclocypris*, *Cypria*, *Cypridopsis*, *Darwinula*) are relatively rare. The following ostracods have been identified (Figs 9, 10): *Candona* cf. *neglecta* Sars [?*Candona* (*Neglecandona*) *paludinica* Krstić], *C. angulata* O.W. Mueller, *Darwinula stevensoni* (Brady et Robertson), *Ilyocypris gibba* (Ramdohr), *I. n bradyi* Sars, *Cyclocypri*s sp. [cf. *C. laevis* (Mueller)], *Prionocypris zenkeri* (Chyzer et Toth), *Metacypris* cf. *cordata* (Brady et Robertson), *Cypridopsis* cf. *vidua* (O.W. Mueller), *Plesiocypridopsis* sp., *Typhlocypris* sp., *Xestoleberis* sp., *Cypria* sp., *Potamocypris* sp., *Candonopsis* sp. and ?*Paralimnocythere* sp. The ostracode valves and carapaces are well preserved (Fig. 10), and it is possible to identify many of their internal (muscle scar pattern, marginal pore system) and external features (sculpture type, nodosity and spines). The specimens are mainly adult forms, whereas juvenile forms (e.g., *Candona*) are scarce.

However, the exact biostratigraphic significance of these ostracod assemblages is unclear. According to the previous studies (Gagić and Sokač, 1972; Krstić, 2006; Krstić *et al.*, 2013), the ostracods in these deposits indicate a transition from the Lower to Middle Paludina Beds, which would mean a slightly younger age than indicated by the

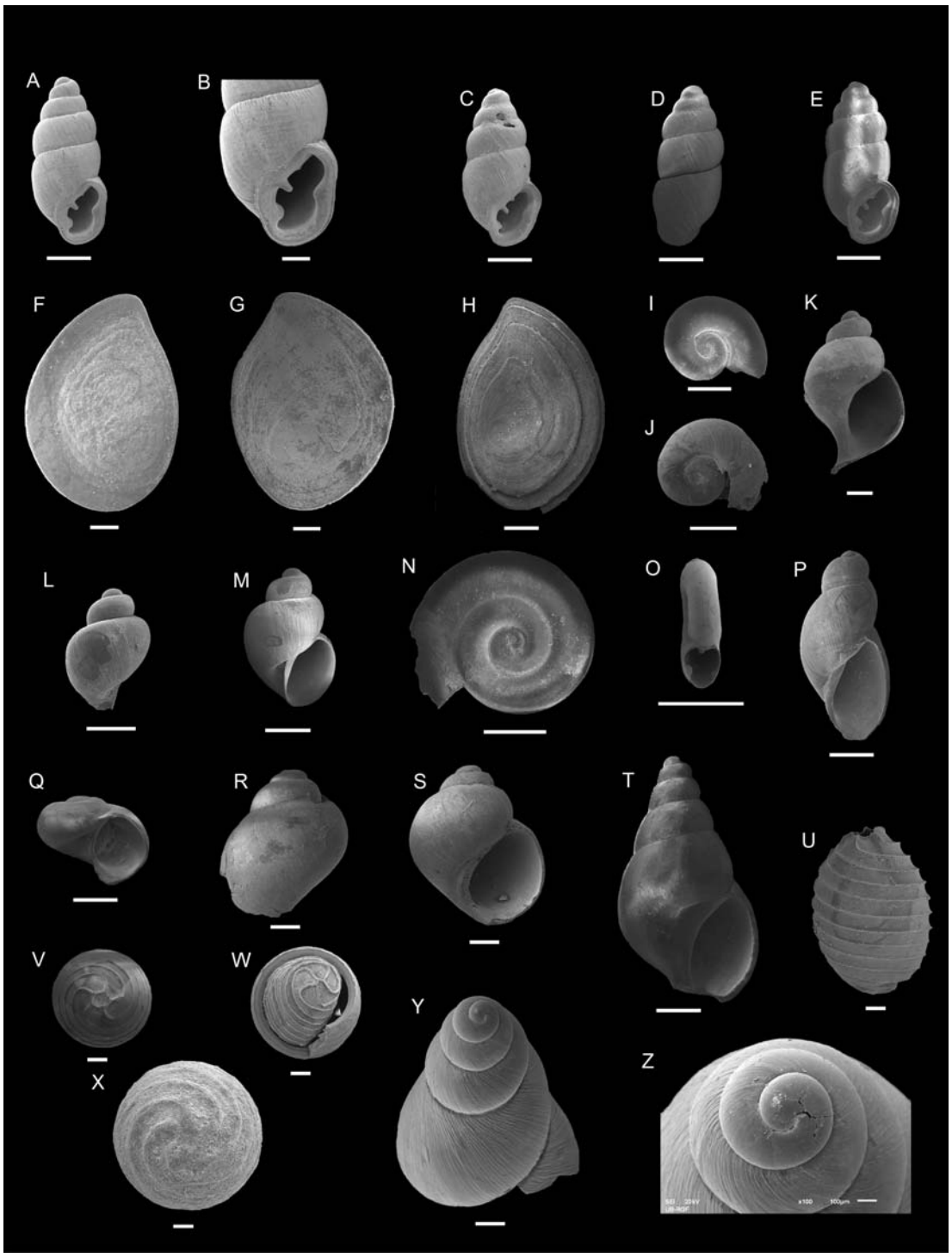

Fig. 8. Small gastropods and charophyte gyrogonites from the lower half of the Sremski Karlovci outcrop section (Fig. 2). **A–E.** *Carychium* sp. from sample SK-2. **F–H.** *Bithynia* sp. (operculum). **I, J.** *Gyraulus* sp. from sample SK-15. **K.** ?*Bithynia* sp. from sample SK-15. **L, M**. Lymnaeidae sp. indet. from sample SK-15. **N.** *Anisus* sp. from sample SK-15. **O.** *Gyraulus* sp. from sample SK-15. **P.** Lymnaeidae sp. indet. from sample SK-15. **Q.** freshwater gastropoda (indet.) from sample SK-2. **R, S.** *Lithoglyphus* sp. from sample SK-15. **T.** *Melanopsis* sp. from sample SK-15. **U–X.** *Chara* sp. (oogonium) from sample SK-3. **Y, Z.** Terrestrial gastropod (indet.) from sample SK-15. The scale bar is 200 μm in cases B, F and G; 100 μm in cases V–X and Z; and 500 μm in all other cases.

molluscs alone. On the other hand, several taxonomic aspects of the subfamily Candoninae (*neglecta* group) remain to be disputed (Meisch and Wouters, 2004; Krstić, 2006). The ostracodes would then seem to indicate that the lower half of the sedimentary succession in the present case (Fig. 2) represents the early Pliocene Dacian Stage.

In addition to the above-mentioned fossil fauna, some of the samples (SK-2, SK-3, SK-8, SK-13 and SK-15, Fig. 2)

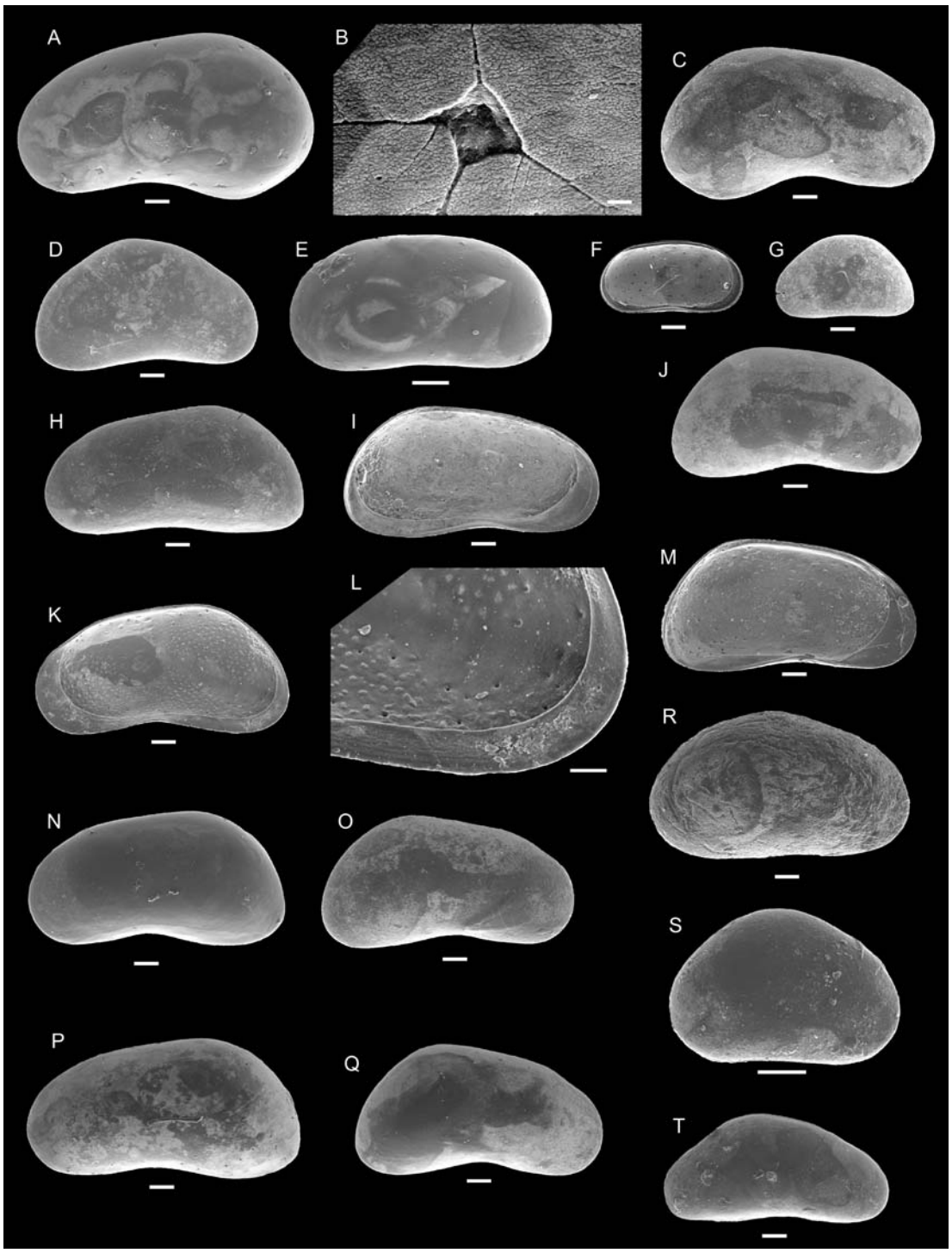

Fig. 9. Ostracods from the lower half of the Sremski Karlovci outcrop section (Fig. 2). **A–C.** *Candona neglecta* Sars, 1887, from sample SK-2: A – right valve, external view, male, length 1.21 mm, height 0.69 mm; B – same specimen, detail of valve ornamentation with pore system; C – right valve, external view, female, length 1.16 mm, height 0.62 mm. **D.** *Potamocypris* cf. *vilosa* (Jurine, 1820), right valve, external view, sample SK-2. **E.** *Herpetocypris* cf. *chevreuxi* (Sars, 1896), left valve, external view, sample SK-2. **F.** *Candona* sp., left valve, internal view, sample SK-2. **G.** *Cypria* sp., left valve, external view, sample SK-2. **H–Q.** *Candona* cf. *neglecta* Sars, 1887, from samples SK-2 and SK-3: H – left valve, external view, female, SK-2; I – left valve, internal view, female, SK-2; J – right valve, external view, female, SK-2; K – right valve, internal view, SK-2; L – same specimen, posteroventral margin; M. Left valve, internal view, female, SK-2; N – left valve, external view, SK-3; O – right valve, external view, SK-3; P – left valve, external view, SK-3; Q – right valve, external view, SK-3. **R.** *Candonopsis* sp., left valve, external view, SK-2. **S.** *Cypridopsis* cf. *vidua (*O.W. Mueller), left valve, external view, SK-2. **T.** ?*Cryptocandona* sp., right valve, external view, SK-15. The scale bar is 100 μm, but is 10 μm in case B and 50 μm in case L.

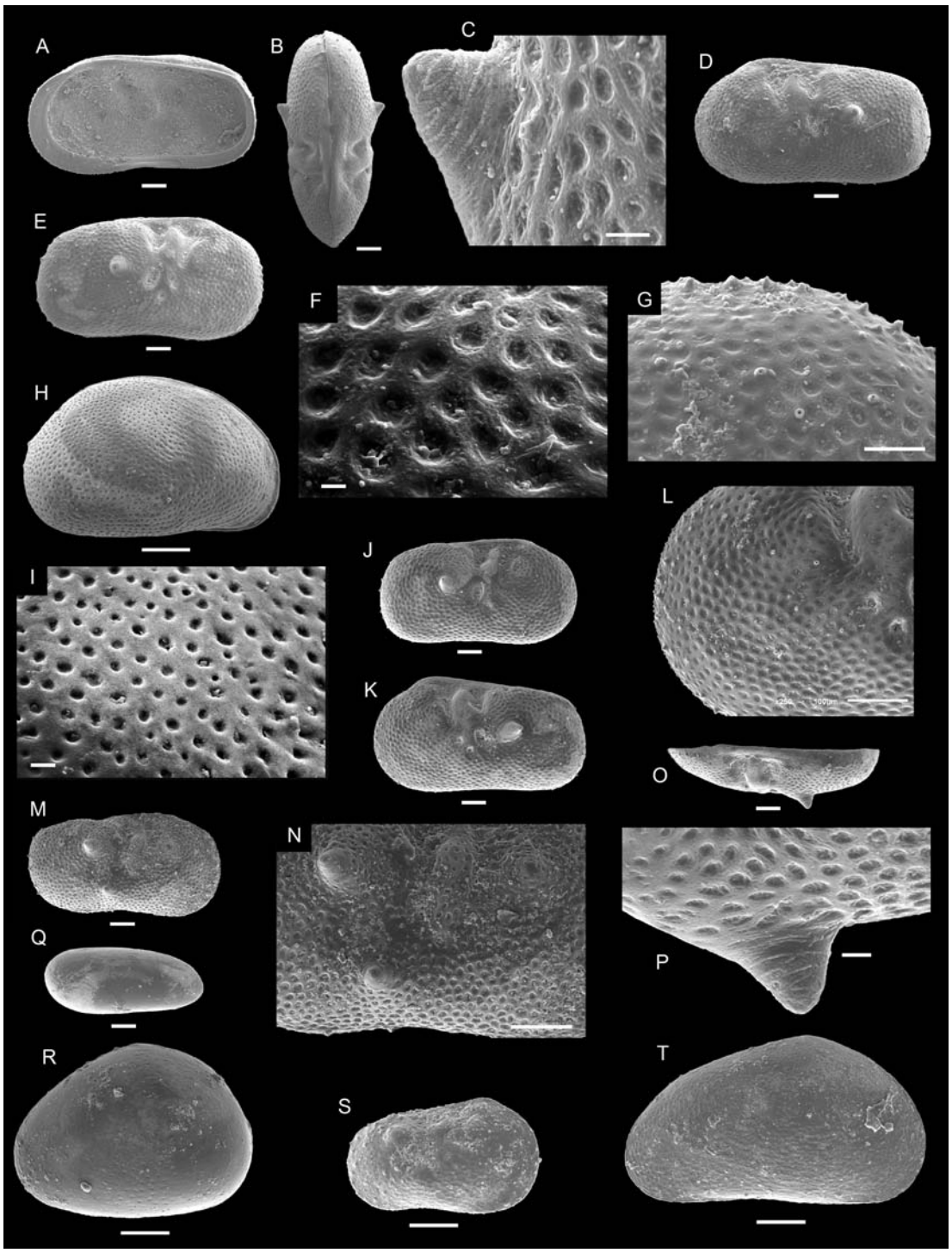

Fig. 10. Other ostracods from the lower half of the Sremski Karlovci outcrop section (Fig. 2). **A–G.** *Ilyocypris gibba* (Ramdohr, 1808) from sample SK-15: A – right valve, internal view; B – carapace, dorsal view; C – carapace, dorsal view, central tubercle; D – left valve, external view; E – right valve, external view; F – same valve, detail of sculpture with pore system; G – same valve, anterodorsal margin with small tubercle. **H.** *Metacypris* cf. *cordata* Brady et Robertson, 1870, from sample SK-14; right valve, external view. **I.** Same valve, detail of sculpture. **J–L**. *Ilyocypris bradyi* Sars, 1890, from sample SK-3: J – right valve, external view; K – left valve, external view; L – same valve, detail of anterior part. **M.** *Ilyocypris* sp. from sample SK-3; right valve, external view. **N.** Same valve, central part with two main tubercles. **O.** *Ilyocypris gibba* (Ramdohr, 1808) from sample SK-15; left valve, dorsal view. **P.** Same valve, the main tubercle. **Q.** *Darwinula stevensoni* (Brady et Robertson, 1870) from sample SK-15; carapace, external view. **R.** *Cypridopsis* sp. from sample SK-2; right valve, external view. **S.** ?*Paralimnocythere* sp. from sample SK-2; right valve, external view. **T.** *Prionocypris zenkeri* (Chyzer et Toth, 1858) from sample SK-15; right valve, external view. The scale bar is 100 μm, but is 10 μm in cases F and I; 20 μm in cases C and P; and 50 μm in case G.

Table 1

Maceral composition (vol.%) and huminite reflectance of sediments samples from the Sremski Karlovci clay pit (sample numbers as in the outcrop log in Fig. 2)

Sample	SK-5 (lignite)	SK-11 (lignite)	SK-12 (clay)	SK-14 (clay)
Textinite	5.1	4.7	7.8	6.6
Ulminite	10.8	10.0	4.4	9.1
Attrinite	12.1	5.7	0.5	9.0
Densinite	20.0	27.4	5.3	12.2
Gelinite	4.9	2.1	0.1	1.1
Corpohuminite	2.6	1.4	0.4	0.8
Total Huminite	**55.5**	**51.3**	**18.5**	**38.7**
Sporinite	6.5	9.0	11.1	1.1
Cutinite	2.8	0.7	7.1	0.5
Resinite	0.5	0.2	0.2	0.2
Suberinite	0.2	0.2	0.0	0.0
Alginite	0.3	0.5	0.0	0.2
Liptodetrinite	6.1	1.1	6.3	4.3
Fluorinite	0.5	0.7	0.0	0.0
Total Liptinite	**16.9**	**12.3**	**24.6**	**6.2**
Fusinite	1.2	8.9	0.2	0.0
Semifusinite	2.5	3.0	0.0	0.0
Macrinite	0.2	0.9	0.0	0.0
Funginite	1.8	6.1	0.0	0.3
Inertodetrinite	7.1	9.8	0.3	0.8
Total Inertinite	**12.7**	**28.8**	**0.5**	**1.1**
Total Mineral	**14.9**	**7.5**	**56.4**	**53.9**
Average huminite reflectance (%)	**0.34±0.03**	**0.32±0.03**	**0.29±0.03**	**0.33±0.03**

appeared to contain fairly abundant gyrogonites of the algae *Chara* and ?*Rhizosolenia*, fish bones, swamp plant remains including fruits and seeds, and a carbonized and/or limonitized plant detritus. Carbonized plant fragments from the families Taxodiaceae and Cupressaceae were found within and near the lignite coal seams, but too poorly preserved to be identified at a genus and species level.

Petrology and geochemistry of organic matter

Maceral composition

The results of huminite reflectance measurements show that the organic matter in the studied sedimentary succession is in the lignitic state of coalification, with a mean random reflectance between 0.29 ± 0.03 to 0.34 ± 0.03 (Table 1; see ISO, 2005).

Huminite is the prevailing maceral group in the lignite samples (up to 50 vol.% in SK-5 and SK-11, Table 1) and in one of the coaly clay samples (38.7 vol.% in SK-14, Table 1). The most abundant macerals are densinite (5.3–27.4 vol.%) and ulminite (4.4–10.8 vol.%), with variable amounts of attrinite (0.5–12.1 vol.%) and textinite (4.7–7.8 vol.%). The contents of gelinite and corpohuminite are low (vol.%). Liptinite content is high (12.3–16.9 vol.%) in the lignite samples and even higher (24.6 vol.%) in one of the coaly clay samples (Table 1). Its most abundant macerals are sporinite (1.1–11.1 vol.%), liptodetrinite (1.1–6.3 vol.%) and cutinite (0.7–7.1 vol.%). Suberinite, alginite, resinite and fluorinite are present in low amounts in all samples. Inertinite content is low in coaly clay samples, but high in the lignite samples (12.7–28.8 vol.%), with inertodetrinite, fusinite, funginite and semifusinite as the main macerals. Macrinite is present in small amounts in all samples.

The content of mineral matter ranges from less than 15 vol.% in lignite to more than 50 vol.% in coaly clay samples (Table 1). Clay and pyrite are the most abundant minerals in lignite samples, and are accompanied by carbonates in coaly clay samples.

Table 2

Organic carbon content and group geochemical parameters of organic matter in sediment samples from the Sremski Karlovci clay pit (sample numbers as in Fig. 2 and Table 1)

Sample	C_{org}^{db} (wt.%)	S^{db} (wt.%)	Extract yield (mg/g C_{org})	Asphaltenes (wt.%)	Alkanes (wt.%)	Aromatics (wt.%)	NSO compounds (wt.%)
SK-5	37.05	3.22	8.74	46.95	8.05	1.40	43.60
SK-11	55.34	1.49	13.86	59.97	2.98	2.16	34.89
SK-12	2.32	0.05	42.25	12.56	10.23	1.32	75.89
SK-14	6.74	0.34	9.02	28.93	16.86	5.79	48.43

C_{org}^{db} – organic carbon content, dry basis; S^{db} – Total sulphur content, dry basis

Group organic geochemical parameters

Organic carbon content (C_{org}^{db}) varies from 2.32% in coaly clay to 55.34% in lignite samples (Table 2). The total sulphur content (S^{db}) in lignite is the range of 0.05–3.22 wt.% (Table 2). The soluble organic matter (bitumen) extract yield ranges from 8.74 to 42.25 mg/g C_{org} (Table 2), which can be attributed to the varied proportion of biogenic and diagenetic compounds. Lignite samples show a low content of saturated hydrocarbons (2.98–8.05 wt.%) and aromatics (1.40–2.16 wt.%), but a high content of asphaltenes (46.95–59.97 wt.%) and NSO compounds (34.89–43.60 wt.%), as expected for an immature terrestrial organic matter (Table 2). Coaly clay samples have a higher content of saturated hydrocarbons and a relatively high content of NSO compounds, but low content of asphaltenes (Table 2).

Molecular composition of organic matter

The main constituents of the saturated fraction in all samples are *n*-alkanes, with a variable amount of diterpenoids and hopanoids (Table 3, Fig. 11). Non-hopanoid triterpenoids, sesquiterpenoids and steroids occur in small amounts. The main components of the aromatic fraction in samples are diterpenoids and non-hopanoid triterpenoids (Table 4). Other components (e.g., sesquiterpenoids, perylene and phenanthrene) are minor.

The *n*-alkanes show high total ion current (TIC) of the saturated hydrocarbon fraction (Fig. 11) and are identified

Table 3

Concentrations and concentration ratios of compounds and compound groups in the sauturated hydrocarbon fraction of sediment samples from the Sremski Karlovci clay pit (sample numbers as in Fig. 2 and Table 1

Sample	*n*-Alkanes	Steroids	Hopanoids	Sesqui-terpenoids	Di-terpenoids	Tri-terpenoids	CPI[a]	Pristane/ Phytane	Ster/Hop[b]	C_{30} Hop-ene/ C_{30} Hopane[c]	C30ββ/C30 (ββ+αβ)[d]	Di/ (Di+Tri) sat[e]
	(μg/g Corg)											
SK-5	57.48	0.03	5.18	N.D.f	19.54	1.70	2.72	1.07	0.005	1.35	0.05	0.92
SK-11	62.53	0.29	4.71	N.D.f	0.52	5.12	2.90	1.37	0.061	1.52	0.08	0.09
SK-12	410.61	0.73	21.66	N.D.f	22.29	4.42	1.86	0.66	0.034	2.47	0.54	0.83
SK-14	243.31	0.51	9.43	2.301	32.38	1.29	4.22	0.83	0.054	42.73	0.31	0.96

[a] CPI – Carbon Preference Index determined for full distribution of n-alkanes C_{23}-C_{33}, CPI = 1/2 [Σodd(*n*-C_{23} - *n*-C_{33})/Σeven(*n*-C_{22} - *n*-C_{32}) + Σodd(*n*-C_{23} - *n*-C_{33})/Σeven(*n*-C_{24} - *n*-C_{34})] (Bray and Evans, 1961);
[b] Ster/Hop = Steroids/ Hopanoids = [Σ(C_{27}-C_{29})($\Delta^2 + \Delta^4 + \Delta^5$)-Sterenes]/[Σ($C_{29}$-$C_{32}$)17α(H)21β(H)- + Σ($C_{29}$-$C_{31}$)17β(H)21α(H)- + Σ($C_{29}$-$C_{31}$)17β(H)21β(H)- + C_{27}17α(H)- + C_{27}17β(H)- Hopanes + Σ(C_{29}-C_{31}) Hop-17(21)-enes + C_{27}-Hop-17(21)-ene +C_{27}-hop-13(18)-ene] (Peters *et al.*, 2005);
[c] C_{30} Hop-ene/C30 Hopane = C_{30} Hop-17(21)-ene/C_{30} αβ-Hopane;
[d] C_{30}ββ/ C_{30}(ββ+αβ) = C_{30}17 (H)21β(H)-Hopane/(C_{30}17β(H)21β(H)-Hopane + C_{30}17α(H)21β(H)-Hopane) (Mackenzie *et al.*, 1981);
[e] Di/(Di+Tri)sat = ΣDiterpenoids/(ΣDiterpenoids + ΣTriterpenoids), calculated from the TIC of saturated fraction, ΣDiterpenoids = (16α(H)-Phyllocladane + Pimarane + Isopimarane + Norpimarane + Norisopimarane + 16α(H)-Kaurane + 16β(H)-Phyllocladane + Norabietane + Isopimaradiene + Pimaradiene), ΣTriterpenoids = (Olean-12-ene + Olean-13(18)-ene + Des-A-olean-12-ene + Des-A-olean-13(18)-ene + Des-A-olean-18-ene + Des-A-urs-13(18)-ene + Des-A-urs-12-ene + Des-A-lupane);
f N.D. – not determined.

Table 4

Concentrations and concentration ratios of compounds and compound groups in the aromatic hydrocarbon fraction of sediment samples from the Sremski Karlovci clay pit (sample numbers as in Fig. 2 and Table 1)

Samples	Sesqui-terpenoids	Di-terpenoids	Tri-terpenoids	Perylene	Phenantrene	Di/(Di+Tri) arom[a]	Di/(Di+Tri)sat + arom[b]
	(μg/g C_{org})						
SK-5	0.06	2.16	4.33	0.11	0.08	0.33	0.98
SK-11	0.08	1.36	5.38	0.13	0.13	0.20	0.87
SK-12	0.79	1.71	3.64	0.17	1.44	0.32	0.99
SK-14	4.86	180.57	8.61	1.35	0.76	0.95	0.94

[a] Di/(Di + Tri) arom = ΣAromatic diterpenoids/(ΣAromatic diterpenoids + ΣAromatic triterpenoids), (Haberer *et al.*, 2006; Nakamura *et al.*, 2010), calculated from the TIC of aromatic fraction, ΣAromatic diterpenoids = (18-Norabieta-6,8,11,13-tetraene + 19-Norabieta-8,11,13-triene + 18-Norabieta-8,11,13-triene + 2-Methyl, 1-(4'-methylpentyl), 6-isopropylnaphthalene + Dehydroabietane + Simonellite + Retene + Sempervirane + Totarane + Hibaene + Ferruginol + 6,7-Dehydroferruginol + 2-Methylretene + 1,2,3,4-Tetrahydroretene), ΣAromatic triterpenoids = (24,25-Dinoroleana-1,3,5(10),12-tetraene + 24,25-Dinoroleana-1,3,5(10),12,14-pentaene + 24,25-Dinorursa-1,3,5(10),12-tetraene + 24,25-Dinorlupa-1,3,5(10)-triene + Pentamethyldecahydro- chrysene + 3,4,7,12a-Tetramethyl-1,2,3,4,4a,11,12,12a-octahydrochrysene + 3,3,7,12a-Tetramethyl-1,2,3,4,4a,11,12,12a-octahydrochrysene + 3,4,7-Trimethyl-1,2,3,4-tetrahydrochrysene + 3,3,7-Trimethyl-1,2,3,4-tetrahydrochrysene + 1,2,4a,9-Tetramethyl-1,2,3,4,4a,5,6,14b-octahydropicene + 2,2,4a,9-Tetramethyl-1,2,3,4,4a,5,6,14b-octahydropicene + 1,2,9-Trimethyl-1,2,3,4-tetrahydropicene + 2,2,9-Trimethyl-1,2,3,4-tetrahydropicene + 1,2,9-Trimethyl-1,2-dihydropicene + Triaromatic des-A-lupane);
[b] Di/(Di + Tri) sat + arom = ΣDiterpenoids + ΣAromatic diterpenoids/(= ΣDiterpenoids + ΣAromatic diterpenoids + ΣTriterpenoids + ΣAromatic triterpenoids), (Bechtel *et al.*, 2002, 2003)

to be in the range of C_{13} to C_{35}. The *n*-alkane pattern in all samples is dominated by long-chain homologues (C_{27}–C_{35}) with a maximum at *n*-C_{29} and a marked predominance of odd over even lengths, indicating a significant contribution of epicuticular waxes. The high content of *n*-alkanes may be related to the high content of liptinite macerals, especially sporinite, cutinite and resinite. Mid-chain *n*-alkanes (*n*-C_{21}–C_{25}), originating from vascular plants, microalgae, cyanobacteria, *Sphagnum* spp. and aquatic macrophytes (Matsumoto *et al.*, 1990; Ficken *et al.*, 2000; Nott *et al.*, 2000), occur in higher amounts in coaly clay (Fig. 11B) than in lignite samples (Fig. 11A). The relatively high content of C_{23} and C_{25} *n*-alkane homologues implies a contribution of aquatic macrophytes to the organic matter. Short-chain *n*-alkanes (*n*-C_{20}), found mostly in algae and microorganisms, are present in low quantities in all samples.

The values of CPI (Carbon Preference Index) range from 1.86 to 4.22 (Table 3), which is consistent with the low rank of the organic matter. Isoprenoids pristane (Pr) and phytane (Ph) occur in a low amount in lignite and a higher amount in coaly clay. Low concentration of pristane and phytane is typical for immature organic matter (e.g., Dzou *et*

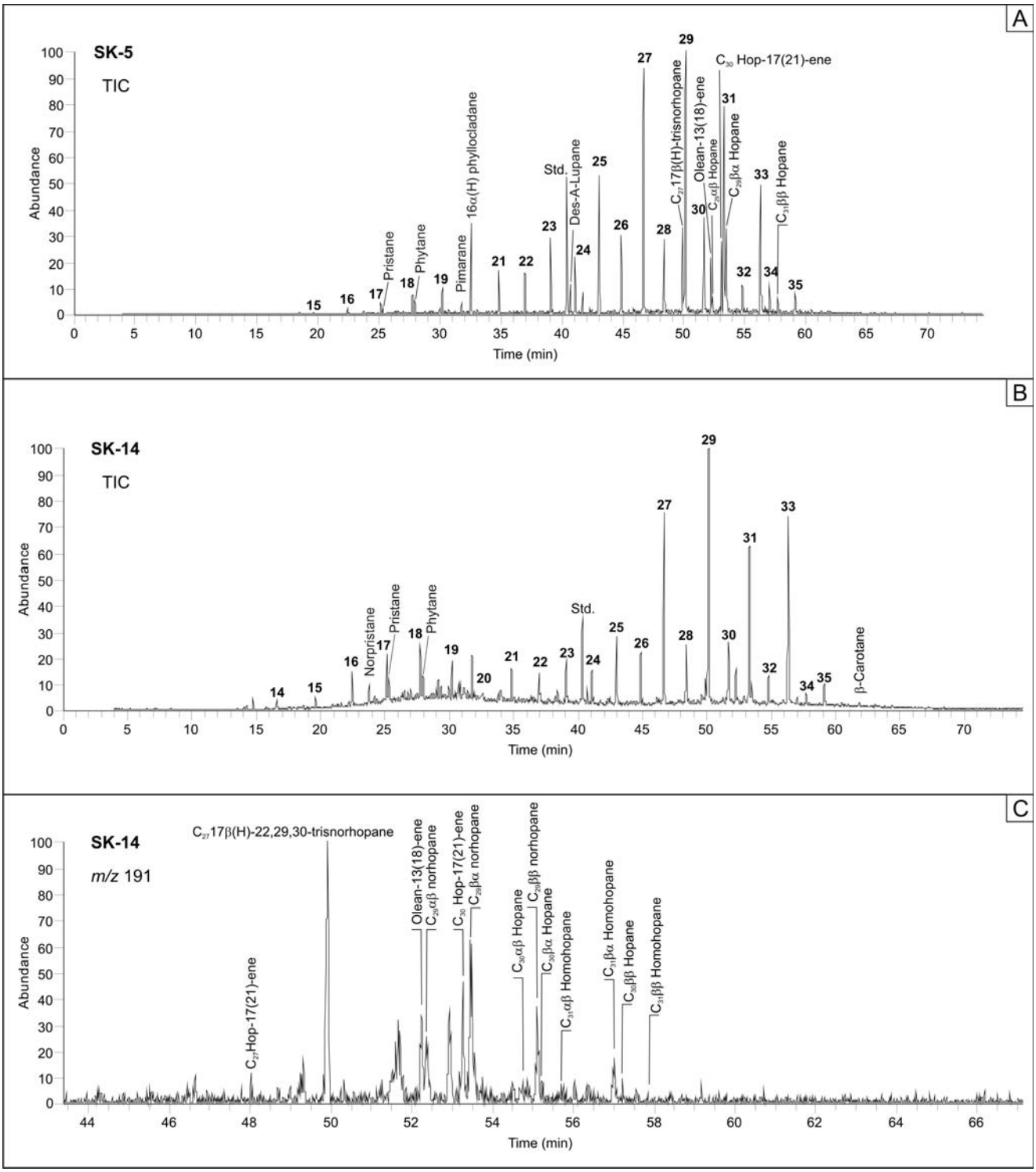

Fig. 11. GC-MS mass chromatograms of TIC (Total Ion Current) of the saturated hydrocarbon fraction of lignite (**A**), coaly clay (**B**) and hopanoids, m/z 191 (C). Peak assignments: *n*-alkanes are labelled according to their carbon number.

al., 1995; Hughes *et al.*, 1995; Vu *et al.*, 2009). The Pr/Ph ratio is widely used as an indicator for the redox conditions in the depositional environment (Didyk *et al.*, 1978), although this parameter is also known to be affected by maturation (Tissot and Welte, 1984) and by differences in the precursors for acyclic isoprenoids of bacterial origin (Goossens *et al.*, 1984; Volkman and Maxwell, 1986; Ten Haven *et al.*, 1987). The influence of maturity on the Pr/Ph ratios can be ruled out in the present case. The Pr/Ph ratios between 0.66 and 1.37 (Table 4) thus seem to indicate a change in redox conditions from anoxic during clay deposition to slightly oxic (Pr/Ph1) during peat accumulation (cf. Didyk *et al.*, 1978). The high inertinite content in lignite samples is consistent with this interpretation.

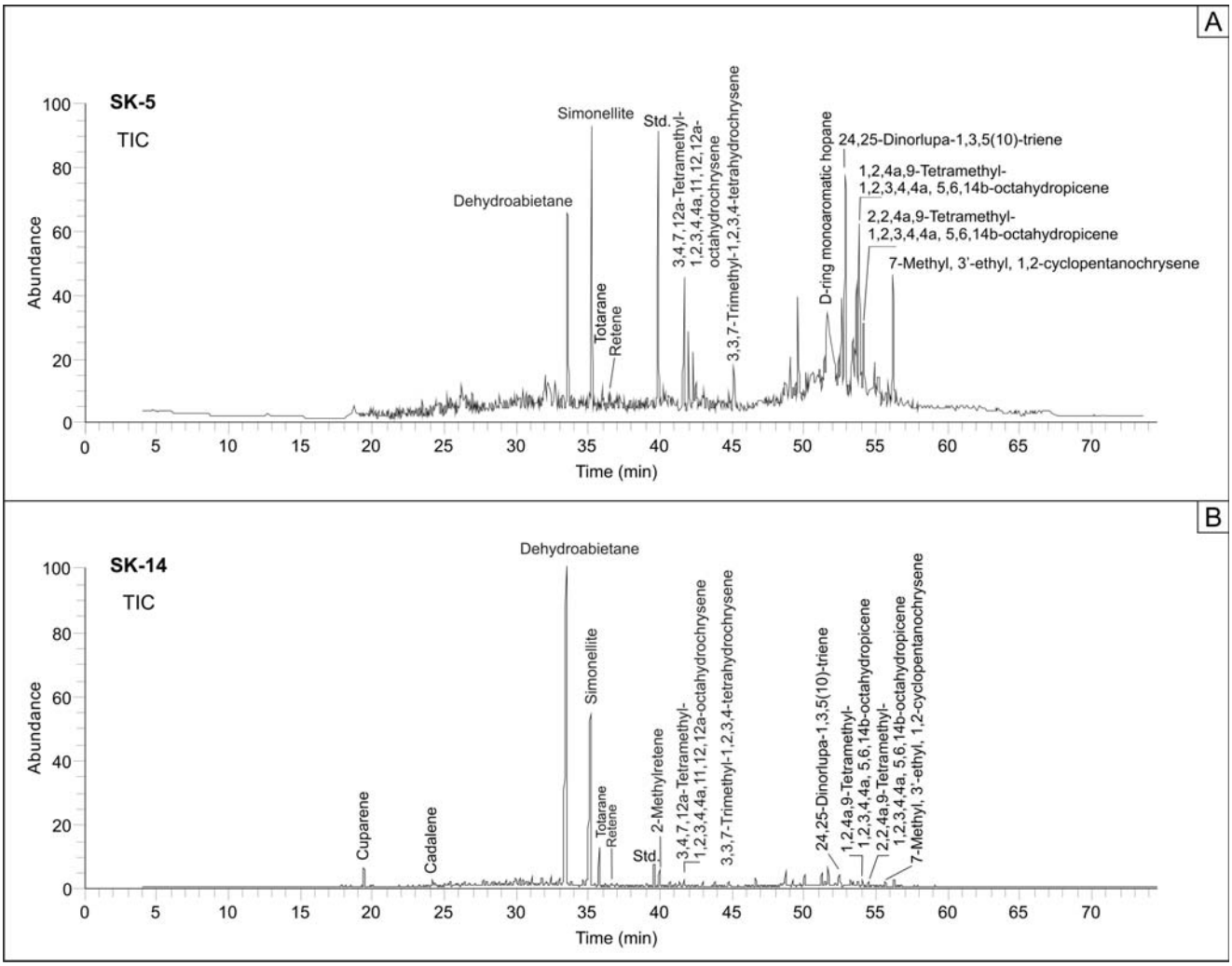

Fig. 12. GC-MS mass chromatograms of TIC (Total Ion Current) of the aromatic hydrocarbon fraction of lignite (**A**) and coaly clay (**B**).

Diterpenoids are present in both saturated and aromatic hydrocarbon fractions, indicating a contribution of gymnosperms to the organic matter. Pimarane and particularly 16a(H)-phyllocladane (Fig. 11A) are the main diterpenoid biomarkers in the saturated fraction. Other diterpenoid constituents of saturated fraction are norabietane, beyerane and isophyllocladane. The presence of 16α(H)-phyllocladane indicates that the peat-forming plants belonged to the conifer families *Taxodiaceae*, *Podocarpaceae*, *Cupressaceae*, *Araucariaceae* and/or *Phyllocladaceae*; the occurrence of pimarane indicates *Pinaceae*, *Taxodiaceae* and/or *Cupressaceae* (cf. Otto *et al.*, 1997; Otto and Wilde, 2001; Stefanova *et al.*, 2002, 2005).

The aromatic diterpenoids consist of abieta-6,8,11,13-tetraenes, dehydroabietane, simonellite, retene, totarane and 2-methylretene (Fig. 12). Dehydroabietane is the dominant aromatic diterpenoid, except for one lignite sample (SK-5) where simonellite is most prominent (Fig. 12A). Almost all aromatic diterpenoids are nonspecific conifer markers, because they are the diagenetic products of a great variety of abietane-type precursors that are common constituents of all conifers except *Phyllocladaceae* (Otto *et al.*, 1997; Otto and Simoneit, 2001; Stefanova *et al.*, 2005). The presence of cuparene and totarane in the aromatic fraction of both lignite and clay extracts indicates a contribution of *Cupressaceae*, *Taxodiaceae*, *Podocarpaceae* and *Araucariaceae* in the biomass (Otto and Wilde, 2001).

The non-hopanoid triterpenoids are present in relatively low amounts in the saturated fraction and include olean-13(18)-ene and des-A-lupane. The related compounds, represented by tetramethylocta and trimethyltetra hydrochrysenes and hydropicenes, are slightly more abundant in the aromatic fraction (Table 4). This evidence indicates that also angiosperms contributed to the organic matter. The higher abundance of aromatized, relative to non-aromatized, angiosperm triterpenoids indicates their aromatization during diagenesis. Aliphatic angiosperm-derived triterpenoids are more readily altered into aromatic derivatives, compared to gymnosperm-derived diterpenoids, which results in a selective loss of such aliphatic compounds (Chaffee *et al.*, 1986; Kalkreuth *et al.*, 1998; Nakamura *et al.*, 2010). The degradation of triterpenoid A-ring followed by intense aromatization suggests microbial activity, consistent with the abundance of hopanoids.

The analysis of aliphatic fraction reveals an extremely low content of steroids (Table 4). Steroid biomarkers con-

sist of C_{29} Δ^3- and Δ^5-sterenes, indicating peat formation from terrigenous plants. The steroids/hopanoids ratio is very low (0.061, Table 3), which implies a bacteria-altered organic matter and suggests a significant role of microorganisms in plant tissue degradation.

Polycyclic alkanes of the triterpane type (m/z 191) are important constituents of alkane fractions. The organic matter in lignite and clay is characterized by the occurrence of ββ-, βα- and αβ-type hopanes from C_{27} to C_{31}, but without C_{28}. The dominant hopane in all samples is $C_{27}17\beta$(H)-22,29,30-trisnorhopane (Fig. 11C). Other constituents are $C_{29}17\beta$(H)21α(H)-norhopane, $C_{29}17\alpha$(H)21β(H)-norhopane, $C_{29}17\beta$(H)21β(H)-norhopane, C_{30}hop-17(21)-ene, $C_{30}17\beta$(H)21α(H)-hopane, and $C_{30}17\beta$ (H)21β(H)-hopane. The ratio of $C_{30}17\beta$(H)21β(H)-hopane to the sum of ($C_{30}17\beta$ (H)21 β(H)-hopane and $C_{30}17\alpha$(H)21β(H))-hopane (Table 4) is within the range generally reported from lignites (Mackenzie *et al.*, 1981). Hopane biomarkers originate from various precursors, such as plants, algae, bacteria and fungi (Peters *et al.*, 2005). The type and abundance of hopanes indicates organic matter degradation by aerobic bacteria. The relatively high content of C_{30}hop-17(21)-ene in clay samples, expressed as the ratio of C_{30}hop-17(21)-ene to C_{30}hopane (Table 4), suggests microbial origin from iron-reducing anaerobic bacteria (Wolff *et al.*, 1992).

The occurrence of a D-ring monoaromatic hopane, 7-methyl, 3'-ethyl, 1,2-cyclopentanochrysene, 4-methyl, 24-ethyl and 19-norcholesta-1,3,5(10)-triene (Philp, 1985) in the aromatic fraction of all samples (Fig. 12) suggests partial aromatization of hopanoids and steroids during diagenesis. This evidence is consistent with the notion of pronounced microbial activity and peatification in a suboxic to oxic environment.

Sesquiterpenoids occur in both saturated and aromatic fractions. In the saturated fraction, they are present in a very low amount in one of the clay samples (SK-14, Table 3). The presence of cadinene and cedrene indicates a contribution of Cupressaceae conifers and dammar resin as precursors to organic matter. Aromatic sesquiterpenoids occur in low quantities in all samples (Table 4). Cadalene predominates over calamenene and cuparene. Sesquiterpenoids are considered to be markers of higher land plants, because they occur in their resinous matter. Cuparene indicates contribution of conifers from the family Cupressaceae, particularly its genera *Cupressus*, *Thuja* and *Juniperus*, as precursors to organic matter (Otto and Wilde, 2001; Haberer *et al.*, 2006), which is consistent with the evidence from palynological data.

Due to an intense aromatization of angiosperm-derived triterpenoids, the ratio of diterpenoids to triterpenoids in saturated fraction, expressed as Di/(Di+Tri)sat in Table 3, is high (>0.80) in three samples, indicating an organic matter composed almost exclusively of conifers. Therefore, to estimate the contribution of gymnosperm and angiosperm vegetation in the peat bogs, this study has used the ratio of diterpenoid and angiosperm-derived triterpenoid aromatic biomarkers (Haberer *et al.*, 2006; Nakamura *et al.*, 2010), given as Di/(Di+Tri)arom in Table 4, and the ratio of total diterpenoids and total non-hopanoid triterpenoids (Bechtel *et al.*, 2002, 2003), given as Di/(Di+Tri)sat+arom in Table 4. The lowest value of this latter parameter in the stratigraphically higher lignite sample (SK-11, Fig. 2 and Table 4) may indicate a temporal increase of angiosperms in the peat-forming vegetation and a dryer and more oxic environment. The lake transgression recorded by lithofacies B (Fig. 2) might then be preceded by a normal highstand regression (Catuneanu, 2006) and coastal swamp expansion – an episode otherwise unrecognizable from lithofacies A in macroscopic terms.

Magnetic mineralogy

Magnetic mineralogy experiments have been conducted on samples of bluish-grey clay from the top of lithofacies B (PM-1, Fig. 2). The IRM acquisition curves (Fig. 13A, B) have a shallow slope for the low strengths of applied magnetic field. With an increase of the applied field, the IRM intensity gradually increases and reaches saturation for a field strength of 300 mT. The curve then assumes a shallow slope at higher applied fields, where most particles are magnetically saturated. This shape of the IRM curves indicates a magnetic fabric of single-domain grains (Roberts *et al.*, 2011). The three component IRM curves (Fig. 13C, D) decline quickly with an increasing temperature and show demagnetization in the temperature range of 375–400 °C, which indicates greigite (cf. Reynolds *et al.*, 1994, 1999; Dekkers *et al.*, 2000).

Greigite is an iron sulfide (Skinner *et al.*, 1964) – a sulfuric equivalent of the iron oxide magnetite – known to be formed in lacustrine deposits by magnetotactic and sulfate-reducing bacteria, possibly as a result of seasonal variation in the composition and physical conditions of lake waters (Anthony *et al.*, 1990; Sagnotti *et al.*, 2010). The susceptibility curves (Fig. 13E, F) show a marked decrease of intensity for temperatures up to 375 °C and further rapid increase. This pattern most probably indicates formation of magnetite by a diagenetic degradation of greigite (Krs *et al.*, 1992) in oxidizing groundwater conditions.

DISCUSSION

Palaeoenvironment and ecological conditions

Most authors in the regional literature agree that the Pliocene Paludina Lake was a freshwater successor to the late Miocene giant Lake Pannon. During the seven million years of its existence (*ca.* 11.6 to 4.5 Ma), the Lake Pannon was gradually filled with clastic sediments and developed a caspibrackish fauna (Magyar *et al.*, 1999, 2013; Sztanó *et al.*, 2013, 2015). In the early Pliocene, the Lake Pannon became a freshwater lake limited to the topographically lowest area of the Pannonian Basin, attracting fluvial drainage brought about by a humid regional 'washhouse' climate (Böhme *et al.*, 2008). The ancestral caspibrackish fauna became replaced by a new freshwater fauna, which explains the moderately high endemicity of Paludina Lake (Magyar *et al.*, 1999). According to Harzhauser and Mandic (2008), the endemism in the Paludina Lake (also known as Lake Slavonia) reaches 63%, with 28 species deriving from the ancestral Lake Pannon and with the high diversity being due to heritage rather than to autochthonous endemic evolution.

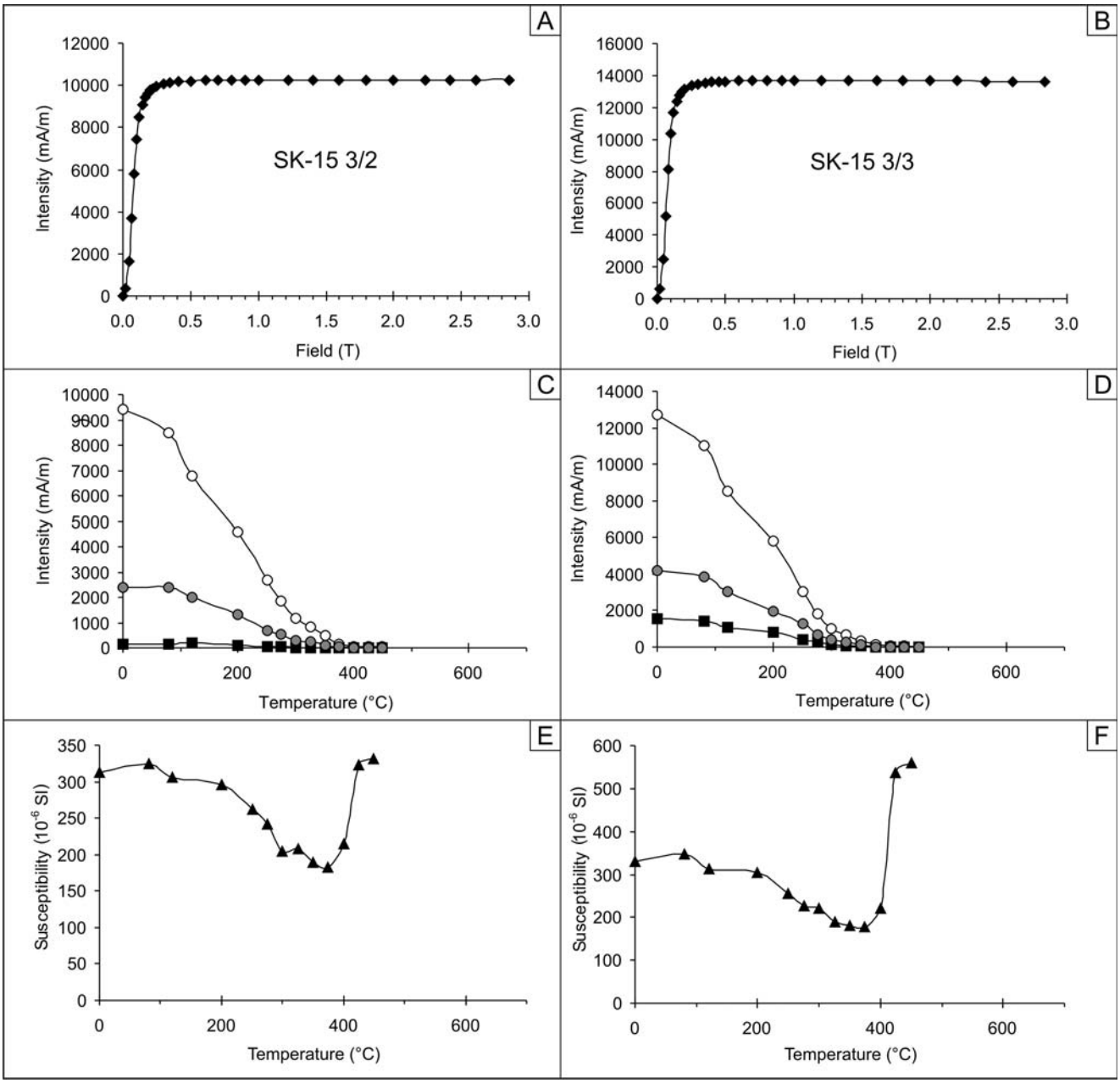

Fig. 13. Magnetic mineralogy experiments on two laboratory subsamples of mud sample SK-15 (Fig. 2); instrumental procedure after Lowrie (1990). **A, B.** IRM acquisition curves. **C, D.** Behaviour of composite IRM during stepwise thermal demagnetization; the high-coercivity (squares), intermediate-coercivity (closed circles) and low-coercivity (open circles) components of the composite IRM were imparted in fields of 2.94, 0.35 and 0.12 T, respectively. **E, F.** Changes in magnetic susceptibility during stepwise thermal demagnetization.

The sedimentary succession in the Sremski Karlovci clay pit (Fig. 2) indicates a lake-margin palaeoenvironment subject to major temporal changes, which are discussed here in terms of the modern concepts of sequence stratigraphy (Catuneanu, 2006; Helland-Hansen, 2009). Lithofacies A in the lowest part of the succession (Fig. 2) indicates an expansion of lake-margin muddy deposits and peat-forming mires over sandy deposits, nearshore/deltaic or possibly terrestrial, which suggests a lacustrine transgressive systems tract. The alternation of clay, mud, silt, fine-grained sand and lignite layers in lithofacies A indicates fluctuating physical conditions, probably due to short-term lake level changes, shoreline oscillations and stepwise increases in accommodation (cf. Morozova and Smith, 2003; Ielpi, 2012; Andreescu *et al.*, 2013). Palaeobotanical evidence from the upper part of lithofacies A indicates an increased terrestrialization, which may imply a cryptic normal-regressive highstand systems tract – unrecognizable from the sedimentary facies alone.

The thick overlying unit of muddy lithofacies B (Fig. 2) indicates drowning of the coastal zone, which means lake major expansion and a transgressive systems tract. The erosional base of coarse-grained lithofacies C (Fig. 2) clearly indicates a forced regression due to the lake level dramatic

fall, with the incision of a fluvial valley ca. 10 m deep and the formation of an inferred delta at the lake lowstand shoreline. The fining-upwards fluvial gravelly sands of lithofacies C are aggradational deposits of incised valley-fill representing a transgressive systems tract. The lake transgression culminated in the deposition of muddy lithofacies D (Fig. 2). The increase in sand content towards its top may be a signature of the transgressive systems tract turning into a normal-regressive highstand tract.

The lake floor in the study area was subsequently emerged, denudated and vegetated, before being covered with Pleistocene loess deposits (Fig. 2). The regional shift to terrestrial environment and semiarid climate apparently changed the groundwater pH into highly oxidizing, which caused the reddening of sediments around a fluctuating groundwater table and the diagenetic transformation of greigite into magnetite at deeper levels.

The diversity and composition of fauna assemblages in the Sremski Karlovci section are comparable to those reported by Harzhauser and Mandic (2008) from the Slavonian part of the palaeolake. There is a notable similarity in the abundance of viviparids, including *Viviparus neumayri*, and many other gastropods, particularly from the genus *Melanopsis*. Species such as *Melanopsis recurens*, *M. lanceolata*, *M.* cf. *slavonica* and *M*. cf. *friedeli* are endemic organisms stemming from the original Lake Pannon. Solitary shells and opercula of the genus *Bithynia* were also found (Fig. 8). Representatives of the pulmonate freshwater gastropod genera *Gyraulus* and *Planorbis* are fairly abundant, but less diversified. Their relative abundance in certain isolated mud layers (samples SK-2 and SK-15, Fig. 2) indicates that these organisms apparently thrived in a specific narrow range of lake physicochemical conditions (cf. Ielpi, 2012). A brief occurrence of specific environmental conditions, such as a storm wave impact on coastal swamps, may also explain the episodic appearance of terrestrial pulmonate *Carychium* in the lake-margin deposits. The occurrence of numerous small forms of *Theodoxus* in lithofacies A supports the notion of freshwater conditions and frequent lake-level changes. *Theodoxus* lives on a coarse-grained substrate to acquire nutrient, but favours a water depth of at least 5–6 m (Anadón *et al.*, 2002). Such specific conditions in a shallow lake occur episodically only during the lake rapid transgression.

Ostracodes in the Sremski Karlovci outcrop section of the Paludina Lake represent a relatively diversified freshwater lacustrine/swamp assemblage, which can be interpreted through a comparison with modern ostracode fauna. The most abundant species in the palaeolake sedimentary succession are *Candona* cf. *neglecta*, *Ilyocypris gibba* and *I. bradyi*. *C. neglecta* has a wide global spread today and is known to prefer relatively cool shallow waters, 5–20 m deep, but can survive for short periods in water temperatures above 20 °C (Meisch, 2000; Wilkinson *et al.*, 2005). This species has been reported also to tolerate low oxygen levels and a salinity range of 0.5–16‰ (Danielopol *et al.*, 1993; Wilkinson *et al.*, 2005; Li *et al.*, 2010). The two species of *Ilyocypris* most common in the present case, *I. bradyi* and *I. gibba*, are similarly known from freshwater streams, ponds and shallow lakes, with a preference for spring-supplied water (Meisch, 2000; Wilkinson *et al.*, 2005). Although *I. bradyi* is generally associated with waters of a very low salinity (oligohaline water, mean salinity 3.24 ‰), it has been also recognized to tolerate water salinity of up to 14‰ (Li *et al.*, 2010). *I. gibba* lives in a wider range of temperatures in oligohaline stagnant or flowing water environments (Meisch, 2000; Wilkinson *et al.*, 2005; Li *et al.*, 2010).

The occurrence of *Chara* indicates a water depth of no more than 5–6 m, and the notion of shallow water is supported further by the presence of such species as *Herpetocypris* cf. *chevreuxi*, tolerating salinity up to 4‰, and *Darwinula stevensoni* (Wilkinson *et al.*, 2005). The presence of *Prionocypris zenkeri* in association with *I. bradyi* implies slow-flowing streams and may indicate spring-water sources near the lake (Li *et al.*, 2010). This inference is supported by the lack of juvenile instars (cf. Steenbrink *et al.*, 2006).

Plant remains and geochemical analysis of organic matter indicate a wetland coast inhabited by peat-forming plants from the gymnosperm families Taxodiaceae, Podocarpaceae, Cupressaceae, Araucariaceae, Phyllocladaceae and/or Pinaceae. The partial aromatization of hopanoids and steroids during lignite diagenesis indicates pronounced microbial activity and a peatification in suboxic to oxic conditions. The peatification of plant detritus in clay involved anaerobic, iron-reducing bacteria. The relatively high amount of charophyte gyrogonites in some clay layers (sample SK-15, Fig. 8) indicates episodic development of *Chara* meadows in the lake nearshore zone. *Chara* meadows in modern lakes are found in oligotrophic to eutrophic/mesotrophic, alkaline waters no deeper than 10 m (Anadón *et al.*, 2002). In the Paludina Lake, *Chara* meadows formed in oligohaline (7‰) waters no deeper than 5–6 m (Krstić, 2006). The organic content of lake mud and the absence of borrowing testify to a perennial water stratification and strongly anoxic bottom waters (Cohen, 2003).

The palaeomagnetic (NRM) study has shed additional light on the diagenetic environment of the lake muddy deposits. The results confirm that the NRM resides in greigite (Lesić *et al.*, 2007), as has been reported also from the muds of Lake Pannon (Babinszki *et al.*, 2007; Márton *et al.*, 2012) and from other Pliocene lacustrine deposits in the Carpathian foredeep (Vasiliev, 2007) and the Mediterranean region (Sagnotti *et al.*, 2010). Greigite is an intermediate ferromagnetic mineral that forms in sulphate-reducing porewater environments as a precursor to pyrite (Roberts and Turner, 1993). The evidence of greigite diagenetic alternation into magnetite supports the notion of a change to oxidizing groundwater conditions after the lake-floor emergence, when also the reddening of sands occurred due to formation of hematite pigment by intrastratal weathering of iron-bearing detrital grains (cf. Walker, 1967, 1973).

The timing of Paludina Lake

The lower half of the studied lacustrine succession (lithofacies A and B, Fig. 2) contains relatively rich fossil fauna, and the presence of smooth-shelled *Viviparus* species (*V. neumayri*) indicates the Lower Paludina Beds of Dacian

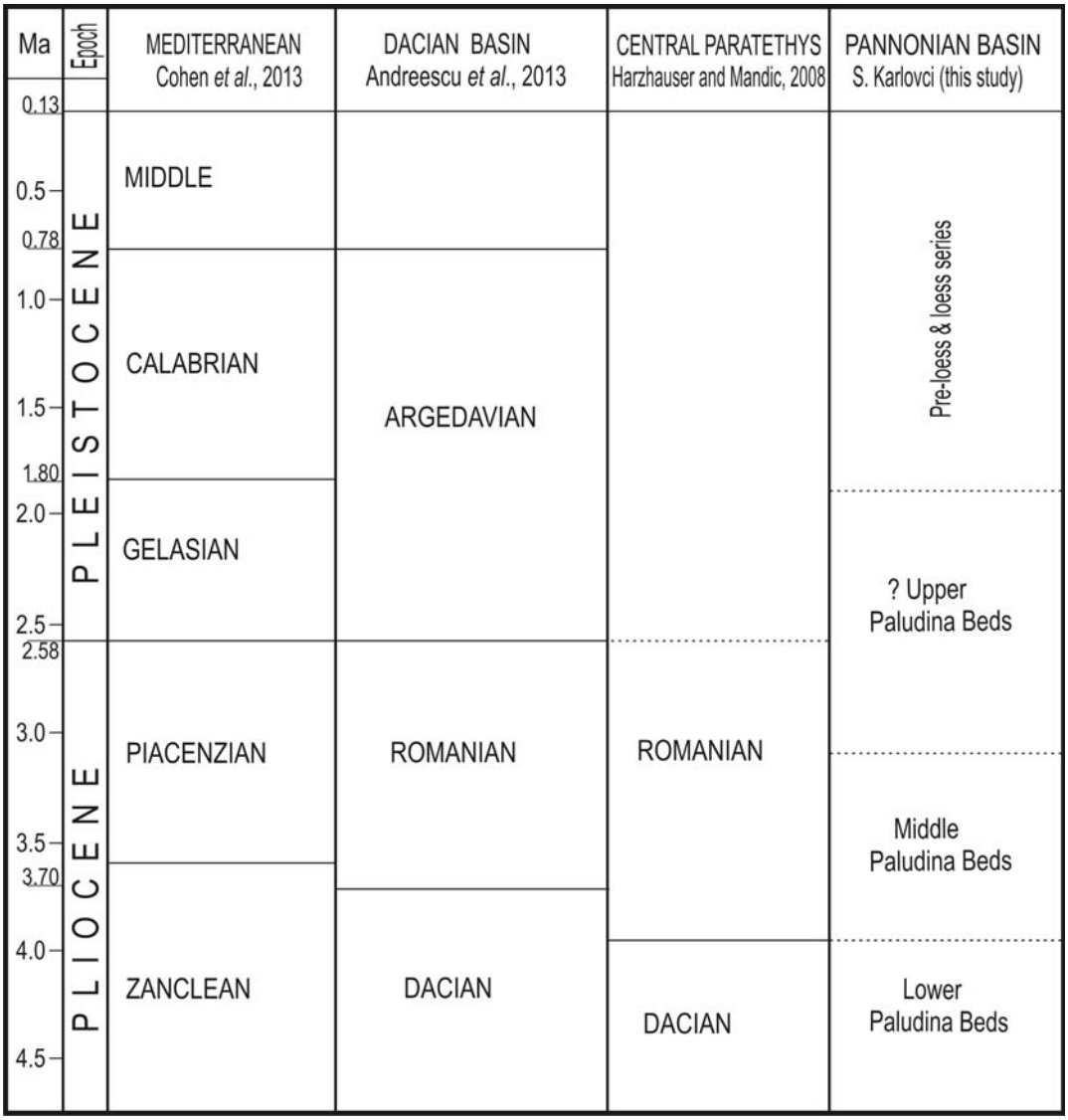

Fig. 14. Chronostratigraphic and biostratigraphic correlation of the Pliocene–Pleistocene in the Mediterranean region, Dacian Basin, Central Paratethys and the present-study area of Pannonian Basin.

age (Fig. 14). Species with a wider stratigraphic range, such as *Melanopsis recurens* and certain ostracodes, suggest a younger part of the Lower Paludina Beds and probable transition to the Middle Paludina Beds (Fig. 14). The gravelly sands of lithofacies C are practically devoid of fossil fauna, and also the overlying lithofacies D (Fig. 2) contains only sporadic planorbid shells and no age-diagnostic fossils. The stratigraphic age of these deposits is thus difficult to determine. It is likely that the upper half of the lacustrine sedimentary succession, overlain by palaeosol and a regional blanket of Pleistocene loess, represents the Middle Paludina Beds and possibly includes also a relic lowest part of the Upper Paludina Beds (Fig. 14).

The presence of Romanian Stage (Fig. 14) is supported by evidence from nearby outcrops on the other bank of the Danube River and from boreholes near the Freedom Bridge in Sremska Kamenica (Fig. 1B; see Krstić, 2006). For example, the core log from borehole BP-2 (Fig. 1B) shows a loess-covered Pliocene succession *ca*. 30 m thick which bears a close lithological similarity to that in the Sremski Karlovci clay pit. The Pliocene fauna found in the core at depth 65–67 m includes gastropods dominated by the ornamented forms of *Viviparus stricturatus* Neumayr and indicates Middle Paludina Beds.

The Upper Paludina Beds have not as yet been identified in the Fruška Gora foot-plain on the right-hand side of the Danube River, but have been recognized in outcrops near the Žeželj Bridge in Novi Sad on the river left-hand bank (Fig. 1B). They consist of interlayered grey to greenish-grey clay and silt, similar to lithofacies D in Sremski Karlovci (Fig. 2), with a fauna including heavily ornamented viviparid shells such as *Viviparus sturi* Neumayr. These deposits are of a latest Romanian or possibly earliest Pleistocene age, preserved beneath the local Quaternary alluvium on a down-thrown fault block. It is uncertain if their relic equivalents are also locally preserved on the uplifted Fruška Gora horst block.

CONCLUSIONS

1. This case study from the Sremski Karlovci clay pit in northern Serbia has contributed to the existing knowledge on the Paludina Lake – the Pliocene freshwater successor of the late Miocene giant caspibrackish Lake Pannon hosted by the Pannonian Basin. The multidisciplinary study has integrated sedimentary facies analysis, sequence stratigraphy, biostratigraphy, palaeontology, palaeobotany, coal petrology, organic geochemistry and magnetic mineralogy to shed new light on the Paludina Lake physicochemical conditions and evolution at its margin in the foot-plain zone of Fruška Gora mountain ridge.

2. The sedimentary succession studied comprises four main lithofacies units. The lowest unit indicates an expansion of alternating muddy lacustrine environment and peat-forming mires over a sandy lake-margin zone, recording a transgressive systems tract with lake-level fluctuations. An increased terrestrialization of plants at the top suggests a poorly recognizable normal-regressive highstand tract. The overlying thick unit of muddy lacustrine deposits indicates coastal drowning by lake major expansion and a transgressive systems tract. The erosional subsequent unit of fluvial gravelly sands is an incised valley-fill indicating forced regression followed by a transgressive systems tract. The lake transgression culminated in the upper muddy unit, whose upward increase in sand content suggests a normal-regressive highstand tract. The lake floor was subsequently emerged, denudated and vegetated, before being covered with Pleistocene loess deposits.

3. The Pleistocene regional shift to terrestrial conditions and semiarid climate apparently changed the groundwater environment into oxidizing, which caused the reddening of sediments around a fluctuating groundwater table and the diagenetic transformation of primary greigite into magnetite at deeper levels – as indicated by magnetic mineralogical analysis. Greigite was formed by magnetotactic and sulfate-reducing bacteria, possibly as a result of seasonal variation in the physicochemical conditions of lake waters.

4. Interpretation of the lake palaeoecological conditions was based mainly on the mollusc and ostracod assemblages. Genus *Melanopsis* dominates among the gastropods, and several of its species (*Melanopsis recurens*, *M. lanceolata*, *M. spirum*, *M.* cf. *friedeli, M.* cf. *herpula*) derive from the pre-existing Lake Pannon. Pulmonate freshwater gastropod genera *Gyraulus* and *Planorbis* form a marsh–lake assemblage indicating quiet lake-margin conditions subject to water-level fluctuations. An oligohaline shallow cool-water environment, no deeper than 5–6 m, is also indicated by the abundance of certain ostracodes, gastropod *Theodoxus* and *Chara*-meadow mats. Ostracod assemblages with *Prionocypris zenkeri* and *Ilyocypris bradyi* indicate an active inflow of spring water. The local water depth during lake transgression maxima was probably no more than 20 m.

5. Palynological analysis indicates abundant weeds and a rich assemblage of swamp plants including Taxodiaceae, Podocarpaceae and Cupressaceae. Maceral analysis of organic matter shows prevalence of huminite, accompanied by rich inertinite in lignite and liptinite in clay. The huminite group is dominated by densinite and ulminite, the liptinite group by sporinite, liptodetrinite and cutinite, and the inertinite group by inertodetrinite, fusinite, funginite and semifusinite. The main sources of organic matter were gymnosperms (conifers) and microbial biomass, with a contribution of angiosperms. The composition of saturated and aromatic diterpenoid hydrocarbons indicates a predominance of the gymnosperm families Taxodiaceae, Podocarpaceae, Cupressaceae, Araucariaceae, Phyllocladaceae and/or Pinaceae in the peat-forming vegetation. The evidence of a diagenetic partial aromatization of hopanoids and steroids in lignite confirms pronounced microbial activity in the peatification process in a humid suboxic to oxic environment.

6. In terms of regional stratigraphy, the occurrence of biostratigraphically significant index species *Viviparus neumayri* Brusina in the lower half of the lacustrine succession indicates the Lower Paludina Beds of Dacian Stage (early Zanclean age). Other gastropods and certain ostracodes indicate transition to the Middle Paludina Beds of the lower Romanian Stage (late Zanclean–early Piacenzian age). The upper half of the succession lacks age-diagnostic fossils and is considered to represent the Middle Paludina Beds, possibly with an erosional relic of Upper Paludina Beds at the top – below the Pleistocene loess cover.

Acknowledgements

The study was conducted through projects 176006, 176015 and 176016 funded by the Ministry of Education, Science and Technological Development of the Republic of Serbia. We are grateful to the Nexe-Group (IGM Stražilovo d.o.o. Sremski Karlovci) for allowing access to their open pit. Special thanks for field support go to the Nexe-Group geologist Katica Popov. We thank also Violeta Gajić and Nenad Malešević (Faculty of Mining and Geology, University of Belgrade) for technical assistance. The manuscript was critically reviewed by Małgorzata Pisarska-Jamroży (University of Poznań) and an anonymous reviewer, who kindly offered constructive comments and helpful suggestions. The revised version of manuscript was further edited and significantly improved by Wojciech Nemec.

REFERENCES

Allen, J. R. L., 1983. Studies in fluviatile sedimentation: Bars, bar-complexes and sandstone sheets (low-sinuosity braided streams) in the Brownstones (L. Devonian), Welsh Borders. *Sedimentary Geology*, 33: 237–293.

Allen, J. R. L., 1985. *Principles of Physical Sedimentology*. Allen and Unwin, London, 272 pp.

Anadón, P., Burjachs, F., Martin, M., Rodriguez-Lazaro, J., Robles, F., Utrilla, R. & Vazquez, A., 2002. Paleoenvironmental evolution of the Pliocene Villaroya Lake, northern Spain: A multidisciplinary approach. *Sedimentary Geology*, 148: 9–27.

Andreescu, I., Codrea, V., Enache, C., Lubenescu, V., Munteanu, T., Petculescu, A., Stiuca, E. & Terzea, E., 2011. Reassessment of the Pliocene/Pleistocene (Neogene/Quaternary) boundary in the Dacian Basin (Eastern Paratethys, Romania). *Muzeul Olteniei Craiova, Oltenia Studii şi comunicări, Ştiinţele Naturii,* 27: 197–220.

Andreescu, I., Codrea, V., Lubenescu, V., Munteanu, T., Petculescu, A., Stiuca, E. & Terzea, E., 2013. New developments

in the Upper Pliocene – Pleistocene stratigraphic units of the Dacian Basin (Eastern Paratethys), Romania. *Quaternary International*, 284: 15–29.

Anthony, J. W., Bideaux, R. A., Bladh, K. W. & Nichols, M. C. (eds), 1990. *Handbook of Mineralogy, Volume I: Elements, Sulphides, Sulphosalts*. Mineralogical Society of America, Chantilly, 265 pp.

Babinszki, E., Marton, E., Marton, P. & Kiss, L. F., 2007. Widespread occurrence of greigite in the sediments of Lake Pannon: Implications for environment and magnetostratigraphy. *Palaeogeography Palaeoclimatology Palaeoecology*, 252: 626–636.

Bada, G., Horváth, F., Dövényi, P., Szafián, P., Windhoffer, G. & Cloetingh, S., 2007. Present day stress field and tectonic inversion in the Pannonian Basin. *Global and Planetary Change,* 58: 165–180.

Balla, Z., 1986. Palaeotectonic reconstruction of the central Alpine-Mediterranean belt for the Neogene. *Tectonophysics*, 127: 213–243.

Basilici, G., 1997. Sedimentary facies in an extensional and deep-lacustrine depositional system: the Pliocene Tiberino Basin, central Italy. *Sedimentary Geology,* 109: 73–94.

Bechtel, A., Gruber, W., Sachsenhofer, R. F., Gratzer, R., Lücke, A. & Püttmann, W., 2003. Depositional environment of the Late Miocene Hausruck lignite (Alpine Foreland Basin): insights from petrography, organic geochemistry, and stable carbon isotopes. *International Journal of Coal Geology,* 53: 153–180.

Bechtel, A., Sachsenhofer, R. F., Gratzer, R., Lücke, A. & Püttmann, W., 2002. Parameters determining the carbon isotopic composition of coal and fossil wood in the Early Miocene Oberdorf lignite seam (Styrian Basin, Austria). *Organic Geochemistry*, 33: 1001–1024.

Böhme, M., Ilg, A. & Winklhofer, M., 2008. Late Miocene "washhouse" climate in Europe. *Earth and Planetary Science Letters*, 275: 393–401.

Brusina, S., 1870. Monographie der Gattung *Emmericia* und *Fossarulus*. *Verhandlungen der kaiserlich-königlichen zoologisch-botanischen Gesellschaft in Wien*, 1870: 925–938.

Brusina, S., 1874. *Fossile Binnen-Mollusken aus Dalmatien, Kroatien und Slavonien nebst einem Anhange. Deutsche vemehrte Ausgabe der kroatischen im Rad der südslav.* Akademie der Wissenschaften und Künste in Agram erschienen Abhandlung. Actienbuchdruckerei, Agram, 143 pp.

Brusina, S., 1878. Molluscorum fossilium species novae et emendatae, in tellure tertiaria Dalmatiae, Croatiae et Slavoniae inventae. *Journal de Conchyliologie*, 1878: 1–10.

Brusina, S., 1882. Orygoceras, eine neue Gasteropoden-Gattung der Melanopsiden-Mergel Dalmatiens. *Beiträge zur Paläontologie Österreich-Ungarns und des Orients,* 2: 33–46.

Brusina, S., 1884. Die Neritodonta Dalmatiens und Slavoniens nebst allerlei malakologischen Bemerkungen. *Jahrbücher der deutschen Malakozoologischen Gesellschaft,* 11: 1–102.

Brusina, S., 1896. Neogenska zbirka iz Ugarske, Hrvatske, Slavonije i Dalmacije na Budimpestanskoj izlozbi. *Hrvatsko Naravoslovno Drustvo*, 9: 98–150. [In Croatian.]

Brusina, S., 1902. *Iconographia Molluscorum Fossilium in Tellure Tertiaria Hungariae, Croatiae, Slavoniae, Dalmatiae, Bosniae, Herzegovinae, Serbiae and Bulgariae inventorum*. Officina Societá Typographicae, Agram, 10 pp.

Catuneanu, A., 2006. *Principles of Sequence Stratigraphy*. Elsevier, Amsterdam, 375 pp.

Chaffee, A. L., Hoover, D. S., Johns, R. B. & Schweighard, F. K., 1986. Biological markers extractable from coal. In: Johns, R. B. (ed.), *Biological Markers in the Sedimentary Record*. Elsevier, Amsterdam, pp. 311–345.

Čičulić-Trifunović, M. & Rakić, M., 1971. *Basic Geological Map 1:100 000, Sheet Novi Sad, with Explanatory Book.* Savezni Geološki Zavod, Beograd, 52 pp. [In Serbian.]

Cloetingh, S., Bada, G., Matenco, L., Lankreijer, A., Horvath, F. & Dinu, C., 2006. Modes of basin (de)formation, lithospheric strength and vertical motions in the Pannonian–Carpathian system: inferences from thermo-mechanical modelling. In: Gee, D. G. & Stephenson, R. A. (eds), *European Lithosphere Dynamics*. *Geological Society of London*, *Memoirs*, 32: 207–221.

Cohen, A. S., 2003. *Paleolimnology*. Oxford University Press, Oxford, 500 pp.

Cohen, K. M., Finney, S. C., Gibbard, P. L. & Fan, J.-X., 2013. The ICS International Chronostratigraphic Chart. *Episodes*, 36: 199–204.

Crenshaw, M. A., 1980. Mechanisms of shell formation and dissolution. In: Rhoads, D. C., Lutz, R. A. (eds), *Skeletal Growth of Aquatic Organisms: Biological Records of Environmental Change*. Plenum Press, New York, pp. 115–132.

Danielopol, D. L., Handl, M. & Yu, Y., 1993. Benthic ostracods in the pre-Alpine deep Lake Mondsee: notes on the origin and distribution. In: McKenzie, K. G. & Jones, P. J. (eds), *Ostracoda in the Earth and Life Sciences*. Proceedings of the 11th International Symposium on Ostracoda, Warnambool (Victoria, Australia). A. A. Balkema, Rotterdam, pp. 465–480.

Dekkers, M. J., Passier, H. F. & Schoonen, M. A. A., 2000. Magnetic properties of hydrothermally synthesized greigite (Fe_3S_4)-II. High- and low-temperature characteristics. *Geophysical Journal International*, 141: 809–819.

Didyk, B. M., Simoneit, B. R. T., Brassell, S. C. & Eglinton, G., 1978. Organic geochemical indicators of palaeoenvironmental conditions of sedimentation. *Nature*, 272: 216–222.

Dzou, L. I. P., Noble, R. A. & Senftle, J. T., 1995. Maturation effects on absolute biomarker concentration in a suite of coals and associated vitrinite concentrates. *Organic Geochemistry*, 23: 681–697.

Ficken, K. J., Li, B., Swain, D. L. & Eglinton, G., 2000. An n-alkane proxy for the sedimentary input of submerged/floating freshwater aquatic macrophytes. *Organic Geochemistry*, 31: 745–749.

Fodor, L., Csontos, L., Bada, G., Györfi, I. & Benkovics, L., 1999. Tertiary tectonic evolution of the Pannonian basin system and neighbouring orogens: a new synthesis of paleostress data. In: Durand, B., Jolivet, L., Horvath, F. & Seranne, M. (eds), *The Mediterranean Basins: Tertiary Extension within the Alpine Orogen*. *Geological Society of London, Special Publication*, 156: 295–334.

Fontannes, F., 1886. Contribution a la fauna malacologique des terrains Neogenes de la Roumanie. *Archives du Muséum d'Historie natturelle de Lyon*, 4: 1–49.

Gagić, N. & Sokač, A., 1970. Ostracod fauna from the Paludina beds of Vukomeričke gorice. Proceedings of VII Congress of Geologists of Yugoslavia, 1: 131–148 [In Serbian.]

Goossens, H., de Leeuw, J. W., Schenck, P. A. & Brassell, S. C., 1984. Tocopherols as likely precursors of pristane in ancient sediments and crude oils. *Nature*, 312: 440–442.

Haberer, M. R., Mangelsdorf, K., Wilkes, H. & Horsfield, B., 2006. Occurrence and palaeoenvironmental significance of aromatic hydrocarbon biomarkers in Oligocene sediments from the Mallik 5L-38 Gas Hydrate Production Research Well (Canada). *Organic Geochemistry*, 37: 519–538.

Harzhauser, M. & Mandic, O., 2008. Neogene lake systems of Central and South-Eastern Europe: Faunal diversity, gradients and interrelations. *Palaeogeography, Palaeoclimatology, Palaeoecology*, 260: 417–434.

Helland-Hansen, W., 2009. Towards the standardization of sequence stratigraphy: Discussion. *Earth-Science Reviews*, 94: 95–97.

Herbich, F. & Neumayr, M., 1875. Beitrage zur Kenntnis fossiler Binnenfaunen, VII. Die Susswasserablagerungen im sudostlichen Siebenburgen. *Jahrbuch der kaiserlich-königlichen geologischen Reichsanstalt*, 25: 401–431.

Horváth, F., Bada, G., Szafian, P., Tari, G., Adam, A. & Cloetingh, S., 2006. Formation and deformation of the Pannonian Basin: constraints from observational data. In: Gee, D. G. & Stephenson, R. A. (eds), *European Lithosphere Dynamics. Geological Society of London*, *Memoir*, 32: 191–206.

Hughes, W. B., Holba, A. G. & Dzou, L. I. P., 1995. The ratios of dibenzothiophene to phenanthrene and pristane to phytane as indicators of depositional environment and lithology of petroleum source rocks. *Geochimica et Cosmochimica Acta*, 59: 3581–3598.

Ichaso, A. A. & Dalrymple, R. W., 2009. Tide- and wave-generated fluid mud deposits in the Tilje Formation (Jurassic), offshore Norway. *Geology*, 37: 539–542.

Ielpi, A., 2012. Anatomy of major coal successions: Facies analysis and sequence architecture of a brown coal-bearing valley fill to lacustrine tract (Upper Valdarno Basin, Northern Apennines, Italy). *Sedimentary Geology*, 265–266: 163–181.

ICCP (International Committee for Coal Petrology), 2001. The new inertinite classification (ICCP System 1994). *Fuel*, 80: 459–471.

ISO, 2009a. *Methods for the Petrographic Analysis of Coals, Part 2: Methods of Preparing Coal Samples*. Publication 7404-2, International Organization for Standardization, Geneva, 12 pp.

ISO, 2009b. *Methods for the Petrographic Analysis of Coals, Part 3: Method of Determining Maceral Group Composition*. Publication 7404-3, International Organization for Standardization, Geneva, 7 pp.

ISO, 2009c. *Methods for the Petrographic Analysis of Coals, Part 5: Method of Determining Microscopically the Reflectance of Vitrinite.* Publication 7404-5, International Organization for Standardization, Geneva, 14 pp.

ISO, 2005. *Classification of Coal*. Publication 11760, International Organization for Standardization, Geneva, 9 pp.

Janković, P., 1970. Paludina Beds in Vojvodina. In: *Proceedings of the VII Congress of Geologists of Yugoslavia*, 1: 103–115. [In Serbian.]

Janković, P., 1977. Paludina Beds. In: Petković, K. (ed.), *Geology of Serbia, Stratigraphy of Cainozoic, Part II-3*. University of Belgrade, Belgrade, pp. 326–330. [In Serbian.]

Janković, P., 1995. Äquivalente der Dazischen Stufe in Vojvodina, Jugoslawien (ältere Paludinenschichten). In: Marinescu, F. & Papaianopol, I. (eds), *Chronostratigraphie und Neostratotypen, Band IX: Dacien*. Academia Română, Bucuresti, pp. 88–92.

Kalkreuth, W., Keuser, C., Fowler, M., Li, M., McIntyre, D., Püttmann, W. & Richardson, R., 1998. The petrology, organic geochemistry and palynology of Tertiary age Eureka Sound Group coals, Arctic Canada. *Organic Geochemistry*, 29: 799–809.

Krs, M., Novak, F., Krsova, M., Pruner, P., Koulikova, L. & Jansa, J., 1992. Magnetic properties and metastability of greigite-smythite mineralization brown-coal basins of the Krusna Hory Piedmont, Bohemia. *Physics of the Earth and Planetary Interiors*, 70: 273–287.

Krstić, N., 2006. *Pliocene Ostracodes of the Paludinian Layers in Pannonian Plain, Serbian Part.* Herald of the Natural History Museum, Belgrade, 401 pp.

Krstić, N. & Knežević, S., 2003. Succession of the fauna of the Paludinian Layers. In: Papaianopol, I., Marinescu, F., Krstić, N. & Macalet, R. (eds), *Chronostratigraphie und Neostratotypen, Neogen der Zentralen Paratethys, Band X: Romanian*. Academia Română, Bucuresti, pp. 83–92.

Krstić, N., Savić, Lj. & Jovanović, G., 2013. The Neogene lakes on the Balkan land. *Annales Géologiques de la Péninsule Balkanique*, 73: 37–60.

Lesić, V., Márton, E. & Cvetkov, V., 2007. Paleomagnetic detection of Tertiary rotations in the Southern Pannonian Basin (Fruška Gora). *Geologica Carpathica*, 58/2: 185–193.

Li, X., Liu, W., Zhang, L. & Sun, Z., 2010. Distribution of Recent ostracod species in the Lake Qinghai area in northwestern China and its ecological significance. *Ecological Indicators*, 10: 880–890.

Lowrie, W., 1990. Identification of ferromagnetic minerals in a rock by coercivity and unblocking temperature properties. *Geophysical Research Letters*, 17: 159–162.

Mackenzie, A. S., Patience, R. L. & Maxwell, J. R., 1981. Molecular changes and the maturation of sedimentary organic matter. In: Atkinson, G. & Zuckermann, J. J. (eds), *Origin and Chemistry of Petroleum*. Proceedings of the 3rd Annual Karcher Symposium. Pergamon Press, Oxford, pp. 1–31.

Magyar, I., Geary, D. H. & Müller, P., 1999 Paleogeographic evolution of the Late Miocene Lake Pannon in Central Europe. *Palaeogeography Palaeoclimatology Palaeoecology*, 147: 151–167.

Magyar, I., Radivojević, D., Sztanó, O., Synak, R., Ujszászi, K. & Pócsik, M., 2013. Progradation of the paleo-Danube shelf margin across the Pannonian Basin during the Late Miocene and Early Pliocene. *Global and Planetary Change*, 103: 168– 173.

Mandic, O., de Leeuw, A., Bulić, J., Kuiper, K. F., Krijgsman, W. & Jurišić-Polšak, Z., 2012. Paleogeographic evolution of the Southern Pannonian Basin: 40Ar/39Ar age constraints on the Miocene continental series of Northern Croatia. *International Journal of Earth Science*, 101: 1033–1046.

Marović, M., Toljić, M., Rundić, L. & Milivojević, J., 2007. Neoalpine Tectonics of Serbia. *Serbian Geological Society*, Belgrade, 87 pp.

Márton, E., Tomljenović, B., Pavelić, D., Pethe, M., Avani, R. & Jelen, B., 2012. Late Miocene clay-rich sediments from the Croatian and Slovenian parts of the Pannonian Basin – paleomagnetisam, magnetic mineral and magnetic fabric. In: Pipík, R. (ed.), *Abstracts and Guide of Excursion, 4th International Workshop on the Neogene from the Central and South-Eastern Europe (Banská Bystrica).* Geological Institute, Slovak Academy of Sciences, Bratislava, pp. 26–27.

Matsumoto, G. I., Akiyama, M., Watanuki, K. & Torii, T., 1990. Unusual distribution of longchain *n*-alkanes and *n*-alkenes in Antarctic soil. *Organic Geochemistry*, 15: 403–412.

Meisch, C., 2000. Crustacea: Ostracoda. In: Schwoerbel, J. & Zwick, P. (eds), *Süßwasserfauna von Mitteleuropa. Band 8(3).* Spektrum Akademischer Verlag, Heidelberg, 522 pp.

Meisch, C. & Wouters, K., 2004. Valve surface structure of *Candona neglecta* Sars, 1887 (Crustacea, Ostracoda). *Studia Quaternaria*, 21: 15–18.

Miall, A. D., 1996. *The Geology of Fluvial Deposits*. Springer-Verlag, Berlin, 582 pp.

Morozova, G. & Smith, N. D., 2003. Organic matter deposition in the Saskatchewan River floodplain (Cumberland Marshes, Canada): effects of progradational avulsion. *Sedimentary Geology*, 157: 15–29

Nakamura, H., Sawada, K. & Takahashi, M., 2010. Aliphatic and aromatic terpenoid biomarkers in Cretaceous and Paleogene angiosperm fossils from Japan. *Organic Geochemistry*, 41: 975–980.

Neumayr, M., 1869. Beiträge zur Kenntniss fossiler Binnenfaunen. *Jahrbuch der Kaiserlich-Königlichen Geologische Reichsanstalt*, 1869/3: 355–382.

Neumayr, M., 1880. Tertiäre Binnenmollusken aus Bosnien und der Hercegovina. *Jahrbuch der Kaiserlich-Königlichen Geologische Reichsanstalt*, 1880: 463–486.

Neumayr, M. & Paul, C. M., 1875. Die Congerien- und Paludinenschichten Slavoniens und deren Faunen. Ein Beitrag zur Descendenz-Theorie. *Abhandlungen der Kaiserlich-Königlichen Geologische Reichsanstalt,* 7: 1–111.

Nott, C. J., Xie, S., Avsejs, L. A., Maddy, D., Chambers, F. M. & Evershed, R. P., 2000. *n*-Alkane distributions in ombrotrophic mires as indicators of vegetation change related to climate variation. *Organic Geochemistry*, 31: 231–235.

Otto, A. & Simoneit, B. R. T., 2001. Chemosystematics and diagenesis of terpenoids in fossil conifer species and sediment from the Eocene Zeitz Formation, Saxony, Germany. *Geochimica et Cosmochimica Acta*, 65; 3505–3527.

Otto, A., Walther, H. & Püttmann, W., 1997. Sesqui- and diterpenoid biomarkers preserved in Taxodium-rich Oligocene oxbow lake clays, Weisselster Basin, Germany. *Organic Geochemistry*, 26: 105–115.

Otto, A. & Wilde, V., 2001. Sesqui-, di-, and triterpenoids as chemosystematic markers in extant conifers – a review. *The Botanical Review*, 67: 141–238.

Peters, K. E., Walters, J. M. & Moldowan, J. M., 2005. *The Biomarker Guide. Volume 2: Biomarkers and Isotopes in the Petroleum Exploration and Earth History*. Cambridge University Press, Cambridge, pp. 475–1155.

Petković, K., Čičulić-Trifunović, M., Pašić, M. & Rakić, M., 1976. *Fruška Gora – Monographic Review of Geological Materials and Tectonic Assembly*. Matica Srpska, Novi Sad, 267 pp. [In Serbian.]

Philp, R. P., 1985. *Fossil Fuel Biomarkers: Applications and Spectra. Methods in Geochemistry and Geophysics*. Elsevier, Amsterdam, 294 pp.

Posilović, H. & Bajraktarević, Z., 2010. Functional morphological analysis of evolution of ribbing in Pliocene viviparid shells from Croatia. *Lethaia*, 43: 457–464.

Potter, P. E., Maynard, J. B. & Depetris, P. J., 2005. *Mud and Mudstones.* Springer-Verlag, New York, 298 pp.

Radivojević, D., Magyar, I., Ter Borgh, M. & Rundić, L., 2014. The Lake Pannon – Serbian side of the story. In: *Proceedings of XVI Serbian Geological Congress*. Serbian Academy of Sciences, Belgrade, pp. 54–60.

Radke, M., Willsch, H. & Welte, D. H., 1980. Preparative hydrocarbon group type determination by automated medium pressure liquid chromatography. *Analytical Chemistry*, 52: 406– 411.

Reynolds, R. L., Rosenbaum, J. G., van Metre, P., Tuttle, M., Callender, E. & Goldin, A., 1999. Greigite as an indicator of drought-the 1912-1994 sediment magnetic record from White Rock Lake. Dallas, Texas, USA. *Journal of Paleolimnology*, 21: 193–206.

Reynolds, R. L., Tuttle, M. L., Rice, C. A., Fishman, N. S., Karachewski, J. A. & Sherman, D. M., 1994. Magnetization and geochemistry of greigite-bearing Cretaceous strata, North Slope Basin, Alaska. *American Journal of Science*, 294: 485–528.

Rögl, F., 1999. Mediterranean and Paratethys. Facts and hypotheses of an Oligocene to Miocene paleogeography. *Geologica Carpathica,* 50: 339–349.

Roberts, A. P., Chang, L., Rowan, C. J., Horng, C.-S. & Florindo F., 2011. Magnetic properties of sedimentary greigite (Fe_3S_4): An update. *Reviews of Geophysics*, 49: 1–46.

Roberts, A. P. & Turner, G. M., 1993. Diagenetic formation of ferrimagnetic iron sulphide minerals in rapidly deposited marine sediments, South Island, New Zealand. *Earth and Planetary Science Letters*, 115: 257–273.

Rundić, L., Vasić, N., Knežević, S. & Cvetkov, V., 2011. The Pliocene sediments from the northern flank of Fruška Gora (northern Serbia) – A new approach based on an integrated study. In: Pipík, R. (ed.), *Abstracts and Guide of Excursion, 4th International Workshop on the Neogene from the Central and South-Eastern Europe (Banská Bystrica)*. Geological Institute, Slovak Academy of Sciences, Bratislava, pp. 38–39.

Sacchi, M. & Horvath, F., 2002. Towards a new time scale for the Upper Miocene continental series of the Pannonian basin (Central Paratethys). *EGU Stephan Mueller Special Publication Series*, 3: 79–94.

Sagnotti, L., Cascella, A., Ciaranfi, N., Marc, P., Maiorano, P., Marino, M. & Taddeucci J., 2010. Rock magnetism and palaeomagnetism of the Montalbano Jonico section (Italy): evidence for late diagenetic growth of greigite and implications for magnetostratigraphy. *Geophysical Journal International*, 180: 1049–1066.

Schmid, S. M., Bernoulli, D., Fügenschuh, B., Matenco, L., Schefer, S., Schuster, R., Tischler, M. & Ustaszewski, K., 2008. The Alpine–Carpathian–Dinaridic orogenic system: correlation and evolution of tectonic units. *Swiss Journal of Geosciences*, 101: 139–183.

Skinner, B. J., Erd, R. C. & Grimaldi, F. S., 1964. Greigite, the thio-spinal of iron; a new mineral. *American Mineralogist*, 49: 543–555.

Steenbrink, J., Hilgen, F. J., Krijgsman, W., Wijbrans, J. R. & Meulenkamp, J. E., 2006. Late Miocene to Early Pliocene depositional history of the intramontane Florina–Ptolemais–Servia Basin, NW Greece: Interplay between orbital forcing and tectonics. *Palaeogeography Palaeoclimatology Palaeoecology*, 238: 151–178.

Stefanova, M., Markova, K., Marinov, S. & Simoneit, B. R. T., 2005. Molecular indicators for coal-forming vegetation of the Miocene Chukurovo lignite, Bulgaria. *Fuel*, 84: 1830–1838.

Stefanova, M., Oros, D. R., Otto, A. & Simoneit, B. R. T., 2002. Polar aromatic biomarkers in the Miocene Maritza-East lignite, Bulgaria. *Organic Geochemistry*, 33: 1079–1091.

Sztanó, O., Szafián, P., Magyar, I., Horányi, A., Bada, G., Hughes, D. W., Hoyer, D. L. & Wallis, R. J., 2013. Aggradation and progadation controlled clinothems and deep-water sand delivery model in the Neogene Lake Pannon, Mako Trough, Pannonian Basin, SE Hungary. *Global and Planetary Change*, 103: 149–167.

Sztanó, O., Sebe, K., Csillag, G. & Magyar, I., 2015. Turbidites as indicators of paleotopography, Upper Miocene Lake Pannon, Western Mecsek Mountains (Hungary). *Geologica Carpathica,* 66: 331–344.

Sykorova, I., Pickel, W., Christanis, K., Wolf, M., Taylor, G. H. & Flores, D., 2005. Classification of huminite-ICCP System 1994. *International Journal of Coal Geology*, 62: 85–106.

Taylor, G. H., Teichmüller, M., Davis, A., Diessel, C. F. K., Littke, R. & Robert, P., 1998. *Organic Petrology*. Gebrüder Borntraeger, Berlin, 704 pp.

Ten Haven, H. L., de Leeuw, J. W., Rullkötter, J. & Sinninghe Damsté, J. S., 1987. Restricted utility of the pristane/phytane ratio as a palaeoenvironmental indicator. *Nature*, 330: 641–643.

Ter Borgh, M., Vasiliev, I., Stoica, M., Knežević, S., Matenco, L., Krijgsman, W., Rundić, L. and Cloetingh, S., 2013. The isolation of the Pannonian basin (Central Paratethys): new constraints from magneto- and biostratigraphy. *Global and Planetary Change*, 103: 99–118.

Tissot, B. T. & Welte, D. H., 1984. *Petroleum Formation and Occurrences.* Second Edition, Springer-Verlag, Berlin, 699 pp.

Toljić, M., Matenco, L., Ducea, M. N., Stojadinovic, U., Milivojević, J. & Đerić, N., 2013. The evolution of a key segment in the Europe–Adria collision: The Fruška Gora of northern Serbia. *Global and Planetary Change*, 103: 39–62.

Traykovski, P., Geyer, W. R., Irish, J. D. & Lynch, J. F., 2000. The role of wave-induced density-driven fluid mud flows for cross shelf transport on the Eel River continental shelf. *Continental Shelf Research*, 20: 2113–2140.

Vasiliev, I., Dekkers, J. M., Krijgsman, W., Franke, C., Longereis, C. G. & Mullender, A. T., 2007. Early diagenetic greigite as a recorder of the paleomagnetic signal in Miocene-Pliocene sedimentary rocks of the Carpathian Foredeep (Romania). *Geophysical Journal International*, 171: 613–629.

Volkman, J. K. & Maxwell, J. R., 1986. Acyclic isoprenoids as biological markers. In: Johns, R. B. (ed.), *Biological Markers in the Sedimentary Record*. Elsevier, Amsterdam, pp. 1–42.

Vu, T. T. A., Zink, K.-G., Mangelsdorf, K., Sykes, R., Wilkes, H. & Horsfield, B., 2009. Changes in bulk properties and molecular compositions within New Zealand Coal Band solvent extracts from early diagenetic to catagenetic maturity levels. *Organic Geochemistry*, 40: 963–977.

Walker, T. R., 1967. Formation of red beds in modern and ancient deserts. *Geological Society of America Bulletin*, 78: 353–368.

Walker, T. R., 1973. Intrastratal alterations in the Fountain Formation (Pennsylvanian age), Denver area, Colorado. *Geological Society of America, Southeastern Section, Abstracts with Program*, 5: 917–920.

Walker, T. R., 1974. Formation of red beds in moist tropical climates: a hypothesis. *Geological Society of America Bulletin*, 85: 633–338.

Walker, T. R. & Honea, R. H., 1969. Iron content of modern deposits in the Sonoran Desert: a contribution to the origin of red beds. *Geological Society of America Bulletin*, 80: 535–544.

Wilkinson, I. P., Bubikyan, S. A. & Gulakyan, S. Z., 2005. The impact of late Holocene environmental change on lacustrine Ostracoda in Armenia. *Palaeogeography Palaeoclimatology Palaeoecology*, 225: 187–202.

Wolff, G. A., Ruskin, N. & Marshall, J. D., 1992. Biogeochemistry of an early diagenetic concretion from the Birchi Bed (L. Lias, W. Dorset, U.K.). *Organic Geochemistry*, 19: 431–444.